This article has been accepted for publication in a future issue of this journal, but has not been fully edited. Content may change prior to final publication. Citation information: DOI 10.1109/RBME.2019.2917780, IEEE Reviews in Biomedical Engineering

A Review of Automated Methods for the Detection of Sickle Cell Disease

Pradeep Kumar Das, *Student Member, IEEE,* Sukadev Meher, *Member, IEEE,*
Rutuparna Panda, *a*nd Ajith Abraham, *Senior Member, IEEE*

***Abstract*—Detection of sickle cell disease is a crucial job in Medical Image Analysis. It emphasizes elaborate analysis of proper disease diagnosis after accurate detection followed by a classification of irregularities, which plays a vital role in the sickle Cell disease diagnosis, treatment planning, and treatment outcome evaluation. Proper segmentation of complex cell clusters makes sickle cell detection more accurate and robust. Cell morphology has a key role in the detection of the sickle cell because the shapes of the normal blood cell and sickle cell differ significantly. This review emphasizes the state-of-the-art methods and recent advances in detection, segmentation, and classification of sickle cell disease. We discuss the key challenges encountered during the segmentation of overlapping blood cells. Moreover, standard validation measures that have been employed to yield performance analysis of various methods are also discussed. The content, in terms of methodologies and experiments, of this review paper is useful to attract researchers working in this area.**

***Index Terms*—Classification, detection, feature extraction, red blood cell (RBC), segmentation, sickle cell disease.**

I. Introduction:

RED BLOOD CELL (RBC) has a significant role in the gaseous interchange of external environment and the living tissue. Haemoglobin is the protein in RBC that works as a carrier of oxygen [1, 63]. Usually haemoglobin A dominates throughout the life after six weeks of age. It contains two alphas and two beta chains [1, 52]. Sickle cell disease (SCD) is found when a person receives two abnormal copies of haemoglobin genes, one from each parent. That means a healthy haemoglobin (HbA) is replaced by sickle haemoglobin (HbS) [1, 52]. We say a person has sickle cell traits if he/she contains single abnormal genes, which means HbS replaces half of the HbA [1]. The life span of healthy RBC is 120 days, whereas that of a sickle RBC is only 10 to 20 days [1].

The shape of RBCs looks sickle like due to the haemoglobin polymerization process of deoxygenated molecule with haemoglobin S [2, 68-72]. Cell morphology has a key role in the classification of the clinical state of the patient [2, 64-67]. The segmentation of cells from the background and count them accurately is a challenging work in the field of biomedicine due to the complex nature of cell [3-7, 73-78]. Proper separation between touching and overlapping cells plays a crucial role in automatic recognition and accurate classification [8-10]. Medical image segmentation becomes more challenging in the presence of non-uniform intensity, noise and diversified signal intensity of lesion cells [11]. The efficiency of the segmentation depends on various characteristics: location, shape, size, area, form factor, elongation, circularity, texture of cell and ellipticity [2, 12-16].

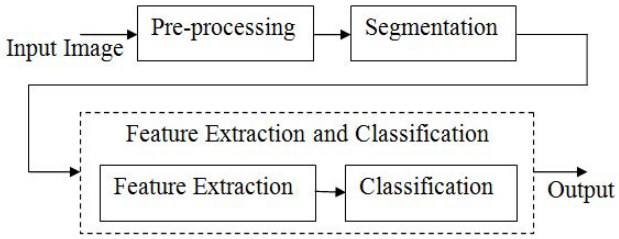

Fig. 1. Schematic of sickle cell detection

Fig. 1 represents the schematic of sickle cell detection. For effective classification, we may employ feature extraction followed by classification step or may apply the technique which performs both feature extraction and classification at a time. The prime motive of the pre-processing step is to boost the image quality. The purpose of the step is to eliminate the unwanted noise and suppress distortions.

The prime objective of segmentation for efficient detection of sickle cell disease is to segregate overlapped cells. It also concentrates on the separation of surrounding blood components (like WBCs and blood plasma) from RBCs and removal of smaller particles like platelets. Sickle cell segmentation can be either manual or automatic. In manual segmentation method, pixels having a similar range of intensities are segmented manually by experienced persons [17, 18]. The performance of this method deteriorates due to unclear boundary, imperfect hand eye coordination and low contrast. This is a subjective process as a segmentation result varies from person to person. It is a very challenging task to extract information on high dimensional and multimodal techniques by using manual segmentation. This problem can be solved by employing automatic segmentation technique [78-82].

This paper mainly focuses on state-of-the-art as well as recent methods of sickle cell segmentation, the problem faced during segmentation and future scope to make the segmen-

P. K. Das and S. Meher are with the Department of Electronics and Communication Engineering, National Institute of Technology, Rourkela 769008, India e-mail: (pdas391@gmail.com; smeher@nitrkl.ac.in).

R. Panda is with the Department of Electronics and Telecommunication Engineering, Veer Surendra Sai University of Technology, Burla 768018, India e-mail: (r_pppanda@yahoo.co.in).

A. Abraham is with the Machine Intelligence Research Labs (MIR Labs), Auburn, WA 98071 USA e-mail: (ajith.abraham@ieee.org).

This article has been accepted for publication in a future issue of this journal, but has not been fully edited. Content may change prior to final publication. Citation information: DOI 10.1109/RBME.2019.2917780, IEEE Reviews in Biomedical Engineering

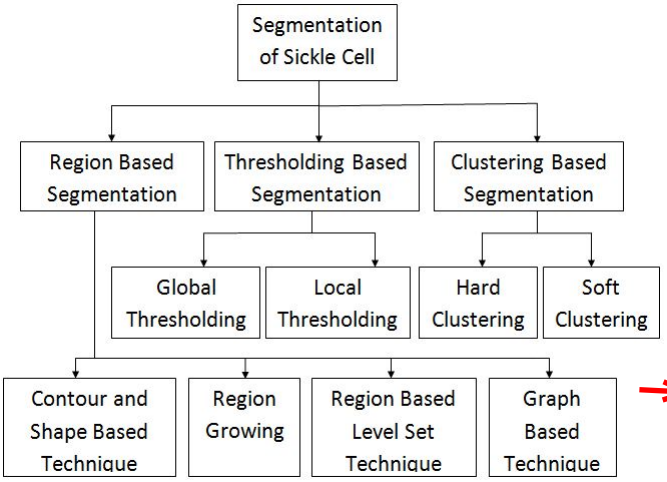

Fig. 2. Sickle cell segmentation techniques

tation more accurate and efficient. We also emphasize on standard validation criteria utilized to measure the performance of the sickle cell segmentation method. The rest of the sections are organized as follows. Section II highlights on various sickle cell segmentation techniques. Section III emphasizes on various feature extraction methods, whereas Section IV provides detailed analysis of classification techniques. Section V discusses the techniques, which are used for both feature extraction and classification purposes. Section VI presents the state-of-the-art validation metrics applied to measure the performance of segmentation methods. Section VII provides a detailed analysis of results. It also highlights on clinical application and hardware implementation. Section VIII emphasizes on future scope of the research. Finally, the paper is summarized and concluded with section IX.

II. Sickle Cell Segmentation Methods

This section mainly focuses on various segmentation techniques, which are applied for segmentation of sickle cell disease. Sickle cell segmentation techniques are mainly categorised into three types: region based segmentation, thresholding based segmentation and clustering based segmentation, as shown in Fig. 2.

A. Region based Segmentation

In region based segmentation technique, homogeneity of intensity has a crucial role in the detection of boundary of an object in an image. This method is further categorised into four types: Contour and shape based technique, Region growing, Region based Level set technique and Graph based technique.

1) Contour and Shape based Technique: In this technique we have to first define a contour, which is similar to the target boundary. It modifies the contour in such a manner that it approaches towards the desire boundary satisfying a predefined criterion. Deformable model (DM) is a popular contour based approach for segmentation of medical image. It begins with arbitrary curves or surfaces, which update itself depending upon the internal and external forces. The internal forces are liable for maintaining smoothness of the model during deformation however, external forces modify the model to achieve desired shape or boundary. Features of an image can be extracted by deforming template [19, 20].

Active contour is either parametric active contour (PAC) [35] or geometric active contour (GAC) [33, 35]. PAC is expressed as a parameterized curve in Lagrangian formulation [21, 32]. GAC is characterized as level set of two-dimensional distance function based on an Euler formula [33, 34]. Snake is a popular energy optimizing active contour, which extracts features like lines and edges. It plays a vital role in motion tracking and stereo matching [21]. Snake is unable to handle topology change in the evolution of curve [62]. Traditional active contour approaches are unable to manage the topological variation of the curve. Level set method emphasises on numerical analysis of shape and surface. It is adaptive to track the shapes that modify topology [21-30]. GAC is preferred over PAC due to its less computational complexity and adaptive nature of curve topology [35]. Level set method may effectively detect contour of Sickle cell image. It not only finds out the cells and cluster of overlapping cell efficiently but also minimises the noise and removes the internal holes [2]. A hybrid geometric deformable technique, which utilises edge based and region based information in a structured manner for segment medical images effectively, has been introduced by Mesejo et al. [31]. As active appearance model (AAM) contains texture information and shape information, it successfully segments RBCs from background [105].

2) Region Growing: It is a technique in which larger region is formed by combing pixels or subregions, which satisfy predefined criteria of growth. Basically, this process starts with a set of seed points. Each seed combines the neighbouring pixels having similar predefined property (similar intensity range, for example) like seed [36-38, 98]. The type of image data and the problem under consideration have a key role in the selection of similarity criteria. Region growing method [133] effectively segments medical images which basically contain object and background. For efficient image segmentation, region growing is combined with edge detection process [36-38]. Cellular automata based segmentation methods automatically choose the seed point to extract retinal blood vessel [39].

3) Region based Level Set Technique : In this method effective contour is derived based on the level set approach [84-87]. It is able to handle topological variations of contour [62]. The energy function of this method is computed by using K means clustering, Fuzzy c means clustering and Gaussian mixture model. A new active contour technique proposed by Chan and Vese [23] is able to detect objects with very smooth boundary. The curve surrounding the desired object is deformed by optimizing the energy function. Unlike classical active contour, it is independent of the gradient of the image. Huang et al. [40] have presented a novel region based method, which is able to segment the image by properly managing intensity inhomogeneities. Energy optimization technique is used for segmentation of image as well as for bias correction [40]. The noise and intensity in-homogeneity can be removed by the local energy extracted from the collective impact on neighbouring pixels. The intensity sharing between desired

This article has been accepted for publication in a future issue of this journal, but has not been fully edited. Content may change prior to final publication. Citation information: DOI 10.1109/RBME.2019.2917780, IEEE Reviews in Biomedical Engineering

object and background, is evaluated by the global energy extracted from the Gaussian model [41].

4) Graph based technique: Nowadays, graph based techniques are widely applied in medical image analysis. The targeted object of a medical image is detected by using both foreground as well as background seeds. For the application of vision (particularly grid graph in vision), min cut and max flow algorithm gives outstanding performance [42]. In the process of random walk every unlabeled pixel should be allocated to corresponding label based on maximum probability to arrive [43]. The presence of noise and non-uniform intensity variation in medical image deteriorate the efficiency of the graph based techniques. The above problem can be solved by using region based statistical model to optimize the statistical region energy with a preceding probability [30].

B. Threshold Based Segmentation

It is the simplest segmentation process, which segments desire objects by comparing the intensity value of each pixel with a threshold value [108]. It is categorized into two types such as global thresholding and local thresholding.

1) Global Thresholding: The global thresholding technique is known as fixed threshold technique as it has a single threshold. Generally, intensity values of pixels greater than or equal to the threshold are considered as objects and the rest are assumed to be background. For example, let an image A(x, y) be segmented based with a threshold value T and let B(x, y) be the resultant binary image after segmentation. The relation between A(x, y) and B(x, y) is thus given by:

$$B(x,y) = \begin{cases} 1, & A(x,y) \geq T \\ 0, & otherwise \end{cases} \quad (1)$$

Segmentation of medical image using the fixed thresholding technique is a challenging job, due to the presence of heterogeneous intensity and noise. So, entropy based fixed threshold techniques are employed for the segmentation of medical image. Otsu's threshold technique is employed to get optimum threshold value automatically [44]. The segmentation of RBC from WBC and platelets is achieved successfully by applying fixed threshold on the saturation image (S of HSV image) as saturation value of RBC differs significantly from that of WBC and platelets [45].

2) Local Thresholding: Local thresholding method adaptively uses different threshold values for each pixel depending upon the intensity information of neighbouring pixels. The local threshold value can be estimated by using previous knowledge, intensity histogram or statistical property like mean intensity value. In medical image processing, thresholding technique is employed for pre-processing, since it is incapable to segment due to the complex nature of medical image [46]. Boegel et al. have proposed a completely automated gradient based adaptive thresholding to segment blood vessel. It first iteratively computes the parameter of fixed thresholding, then apply adaptive thresholding, based on the computed parameters [47].

Thresholding can also be classified as manual thresholding or adaptive thresholding depending upon the selection of the threshold value. In manual thresholding, the threshold value is selected based on prior knowledge or some trial experiment. It is very difficult to accurately segment targeted object from medical image by using the manual thresholding. On the other hand, an adaptive thresholding technique automatically estimates the threshold value depending upon image information and therefore, is more accurate. It can be classified as edge based thresholding, region based thresholding and hybrid thresholding based upon the way of defining the threshold value by analysing image information [51].

The selection of threshold values in an edge-based threshold technique depends upon the edge information about the image. For example, Cany [49], Sobel [1] and Laplacian [48] edge detections may be employed for the purpose. Second derivative information on pixel intensity has a crucial role in the estimation of the threshold value in Laplacian edge detection [48]. In Canny edge detection technique, detection of the potential edge is based on gradient magnitude information. However, suppression of it is based on non-maximal suppression and hysteresis threshold [49]. Rakshit and Bhowmik [1] have employed Sobel operator for the detection of the sickle cell from RBC. They concentrate on high spatial frequency to detect the edge. They estimate the gradient magnitude at each pixel, which has a key role in sickle cell segmentation [1]. The gradient of region boundary has a significant role in region-based thresholding approach [50].

The hybrid thresholding technique is emphasized on proper segmentation of targeted object by combining diverse image information. For example, the combination of watershed segmentation and morphological operation is used to enhance the performance of segmentation [51]. Fadhel et al. [52] have employed watershed segmentation to segment the overlapping cells in RBC image. It has a key role in effective detection of sickle cell anemia [52]. Sharif et al. [53] have applied a marker-controlled watershed technique to segregate the overlapping cells. Before that, they emphasized on the elimination of WBC based on color-conversion, masking, and morphological operations. Platelets are removed by employing morphological operations [53].

C. Clustering Based Segmentation

Clustering is a technique in which objects are combined together with groups based on similarity characteristics like intensity, distance, and connectivity. Clustering can be either hard clustering or soft clustering.

1) Hard Clustering: Hard clustering is a process in which objects or pixels either belong to a cluster completely or do not belong to the cluster. K-Means clustering technique is a hard clustering as well as unsupervised learning technique [54, 98-101]. K-Means clustering can be applied for the segmentation of blood image as blood image has a bimodal histogram. It generates K cluster by combining each object or pixel with nearest mean [54]. Hidalgo et al. [2] have presented a cluster separation technique to detect the SCD. They have applied the ellipse adjustment technique to accurately detect cell [2].

2) Soft Clustering: Soft clustering is a process in which each pixel or object has a probability or likelihood to belong

This article has been accepted for publication in a future issue of this journal, but has not been fully edited. Content may change prior to final publication. Citation information: DOI 10.1109/RBME.2019.2917780, IEEE Reviews in Biomedical Engineering

to a particular cluster. Most popular soft clustering techniques are fuzzy c-means (FCM) and statistical mixture model. FCM is a clustering technique, which permits a pixel or an object to belong to multiple clusters [11, 55]. It uses a membership function to specify whether a pixel lies in a cluster or not. However, its magnitude specifies the degree of membership of a pixel in a cluster [55, 98, 102]. FCM segments pixels into clusters depending on similarity criteria. Thus, it is unable to segment medical image efficiently due to the presence of intensity inhomogeneity, noise and heterogeneous intensity of unhealthy tissue [55]. This problem can be solved by using modified FCM. Chung et al. [55] have presented a modified FCM in which membership functions are modified based on spatial information. It is preferred over traditional FCM as it improves the performance of segmentation by suppressing the intensity inhomogeneity and eliminating noisy spot [55].

The performance of segmentation in medical image processing can be improved by using a statistical mixture model. It evaluates the probability of distribution based on maximum likelihood (ML) or MAP (maximum a posterior) criteria [11]. Gaussian mixture model (GMM) evaluates the pixel intensity based on Gaussian distribution [11]. It is an efficient statistical technique. Here exception maximization based ML is applied to evaluate the probability distribution [11]. Liu and Zhang [116] have suggested an effective local GMM approach for the image segmentation. This method [116] adaptively estimates regularization factor depending upon cost function variation. It is able to give good performance even if in the presence of noise and heterogenous intensity [116]. However, it has certain limitation like over-fitting. MAP approach gives superior performance than ML if it has prior information of an image. Computational complexity is a major drawback of popular statistical mixture models like GMM and hidden Markov random field [11].

III. Feature Extraction

This section highlights on various feature extraction techniques, which are applied to extract suitable features. Most of the authors use morphological features to classify RBCs for the diagnosis of sickle cell disease [52, 56]. Extensively used morphological features are aspect ratio, effect factor, sphericity, RFactor, roundness, and solidity.

Aspect ratio is defined as the ratio of major axis length (M) to the minor axis length (L) of a cell [56, 131, 137]. It is also known as eccentricity [56, 131, 135, 137]. Aspect ratio of a healthy RBC is approximately 1 or slightly greater than 1 whereas an aspect ratio of sickle cell is much larger than 1 [56]. Mathematically aspect ratio is represented as:

$$Aspect\ ratio\ = \frac{M}{L}. \tag{2}$$

Effect factor [56] or metric value [1, 52, 135] is a measure of a cells roundness. It is also known as circular shape factor [69], circularity [131, 137] or form factor [129]. Mathematically effect factor is represented as:

$$Effect\ factor\ = \frac{4\pi \times Area}{Perimeter^2}. \tag{3}$$

Effect factor of healthy RBC is approximately 0.9 whereas that of sickle cell is smaller than 0.4 [52].

Here sphericity [131] indicates the closeness between a cell and the perfect sphere. It is expressed as:

$$Sphericity\ = \frac{Inscribed\ circle\ radious}{Enclosing\ circle\ radious}. \tag{4}$$

RFactor [131] can be represented as:

$$RFactor = \frac{Convex\_Hull}{\pi \times M}. \tag{5}$$

where, $Convex\_Hull$ represents the smallest polygon with fitted-region. Solidity is the ratio of area to the convex area of a cell [128, 131]. It is expressed as:

$$Solidity = \frac{Area}{Convex\_Area}. \tag{6}$$

The prime objective of feature extraction is to extract features of the textures of ROIs (Region of interests). Sharma et al. [56] employ morphological and statistical features like aspect ratio, metric value, variance and radial signature to detect sickle cell anemia and thalassaemia. Fadhel et al. [52] have used effect factor as a feature to detect sickle cell. Tomari et al. [57] estimates compactness and seven Hu moment features [61] for the classification of RBCs.

The feature can also be extracted using classical feature extraction techniques like Gabor filter [115], Discrete wavelet transform (DWT) [104, 113], gray level run length matrix [90], gray level co-occurrence matrix [90], etc. The presence of noise, intensity inhomogeneity along with high dimensional features makes feature extraction more critical. Linear discriminant analysis (LDA), Principal component analysis (PCA) [102, 115], etc. choose the most suitable and optimized features. Hence, it enhances the classification performance.

IV. Classification

The selected or extracted features have been used for classification using K-Nearest Neighbour (KNN) [56, 103, 109, 115, 136], Support Vector Machine (SVM) [99, 101, 102, 109, 111, 115, 135, 136], Artificial Neural Network (ANN) [57, 109-112] or Self organising feature mapping [114]. The main goal of a classifier is to effectively classify the given data with superior performance. KNN detects Sickle cell, elliptocytes, and dacrocytes successfully from RBC which has a significant role in the diagnosis of sickle cell anemia and thalassemia [56]. KNN is one of the simplest non-parametric machine learning methods [56, 127, 136]. It is an instance-based learning technique, which updates the function locally. Sharma et al. [56] have employed KNN to classify sickle cells, dacrocytes, ovalocytes, and healthy erythrocytes. It achieves 80.6% classification accuracy [56]. Tomari et al. [57] have applied ANN classifier for classification of RBCs as well as identification of healthy, sick and overlapping cells [57]. ANN is a supervised machine learning technique, which optimizes the cost function by updating weights [57]. Here Levenberg-Marquardt algorithm is used to train feature vectors, which uses mean squared error as a cost function [57].

This article has been accepted for publication in a future issue of this journal, but has not been fully edited. Content may change prior to final publication. Citation information: DOI 10.1109/RBME.2019.2917780, IEEE Reviews in Biomedical Engineering

Khalaf et al. [59] have applied various machine learning techniques: Random Oracle Model (ROM) [117], Levenberg-Marquardt Neural Network (LEVNN) [118], Trainable decision tree classifier (TREEC) [119], Random Forest classifier (RFC) [120], Functional Link Neural Network (FLNN) [121], Linear combiner Network (LNN) [83], hybrid classifiers H1 and H2 to classify the medical datasets for deciding suitable medication dosages of sickle cell patients [59].

ROM [117] is an ensemble classifier. It is developed by a pair of classifiers and the random oracle [88]. Training data are divided into two groups based on random oracle. ROM is emphasized in the training of a classifier using each group of data. For testing purpose, it applies random oracle to choose a classifier between the pair of classifiers. Then the classifier is applied to classify the data [88]. LEVNN employs a Levenberg-Marquardt (LM) algorithm to train the dataset efficiently [59]. LM algorithm is based on Gauss-Newton [89, 94] and steepest-descent method [89, 94]. It is relatively more stable than Gauss-Newton algorithm and faster than steepest-descent technique. LM algorithm can efficiently use to train a neural network of small and medium size. However, for large network it is not preferred since it requires huge time for the estimation of matrix inversion and Jacobian matrix [122].

TREEC [119] has two stages: growth and pruning stage. The growth stage is emphasized on the iterative splitting of training-dataset depending upon the regional optimal condition [119]. The pruning stage is focused on the elimination of outliers and noise. It can solve the over-fitting problem and also improve the accuracy. The pruning stage is faster compared to the growth stage [119]. FLNN [121] is a flat network, which has no hidden layer. It is a single-layer-feed-forward network. It can be efficiently employed for function approximation and classification purposes [123]. The functional expansion can enhance the dimensionality of the input-vector. Thus, hyperplane developed by an FLNN has superior discrimination ability. It is faster and computationally efficient than multilayer Perceptron [123]. RFC is a supervised learning technique. It generates a group of decision-trees for each randomly selected subgroup of the training dataset. It can effectively classify particles based on votes from various decision-trees [124].

LEVNN and RFC are hybridized with the help of the Levenberg neural network to produce the H1 model [59]. H2 classifier is a hybrid model of RFC and Levenberg-Marquardt learning neural network based on Fischer discriminate analysis [59]. The ROM is applied for random guessing baseline. LEVNN, TREEC, and RFC are nonlinear comparison models. On the other hand, LNN is a linear comparison model, whereas H1 and H2 are applied as a testing model. The performance of H2 is better than any other classifier used in [59].

Extreme learning machine (ELM) is an efficient machine-learning algorithm. It is a feed-forward neural-network, which restrict over-fitting problem [135, 136]. Healthy- and sickle-cells can be successfully classified by employing KNN, SVM, and ELM classifier [135, 136]. Moreover, the classification-performance can be further improved by employing ensemble-learning. It demonstrates superior performance by combining the prediction of individual classifiers [131]. Maity et al. [131] have employed ensemble-learning to efficiently classify RBCs.

V. Feature Extraction and Classification

In this section, we discuss various deep learning techniques, which can be efficiently used for both feature extraction and classification. Deep learning methods like Deep Convolutional Neural Networks (CNNs) [60] and Recurrent Neural Networks (RNNs) [58] can be implemented for accurate and reliable feature extraction and classification of biomedical datasets of sickle cell disease, which will help a physician in disease diagnosis and treatment planning. Both CNNs and RNNs are supervised learning techniques and both of them need large amounts of training data [91]. The patterns of a medical image can efficiently be identified and classified with high accuracy using deep learning techniques [92-97]. Since in CNNs spatial relationship is retained while filtering the images, it becomes more popular in medical image analysis [91]. Xu et al. [60] have proposed efficient Deep CNNs to classify RBCs into five classes such as Echinocytes, Discocytes or Oval, Elongated or Sickle, Reticulocytes and Granular with high accuracy. The Deep CNNs can efficiently classify sickle cells, which can help to detect sickle cell anemia [60, 132, 133].

Khalaf et al. [58] have utilized three types of RNN architecture: Jordan Neural Network Classifier (JNNC), Elman Neural Network Classifier (ENNC) and a hybrid Elman-Jordan Neural Network Classifier (EJNNC) for accurate and reliable classification of Sickle cell dataset. It will help a doctor in treatment planning specifically in deciding the suitable quantity of medication dosage [58].

VI. Validation Measures

Validation measure has a significant role in the quantitative performance analysis of a method as well as finding the limitation of the method. In this section, we highlight the image, database, and performance measures.

A. Image

For sickle cell detection/ segmentation/ classification, the input data is an image of red blood cells. Gonzalez-Hidalgo et al. [2] have employed three types of images: real image, artificial image, and synthetic image.

1) Real Image: Validation of segmentation/ classification using the real image is an appropriate method to ensure the reliability of the technique. Here the real image is the microscopic blood image taken from human beings that contain red blood cells. Real image may contain WBCs, platelets, and noise. Hence, before doing segmentation or classification real image should be pre-processed to enhance the image quality. To boost the segmentation accuracy, we should focus on the elimination of WBCs, platelets, and noise.

2) Artificial Image: We can automatically develop an artificial image using computer code rather than using a real scanner. However, it is impossible to develop a perfect real image using computer code in an artificial manner.

3) Synthetic Image: Synthetic images are developed from real isolated cells, which contains few cells.

Since the artificial and synthetic images are only concentrated to check the validity of the proposed method, most of the researchers have emphasized only the real image for the segmentation/ classification of RBCs.

This article has been accepted for publication in a future issue of this journal, but has not been fully edited. Content may change prior to final publication. Citation information: DOI 10.1109/RBME.2019.2917780, IEEE Reviews in Biomedical Engineering

B. Database

ErythrocytesIDB is a standard database [2], which is available at //erythrocytesidb.uib.es/. It contains 196 full field images and 629 individual cell images (circular, elongated or other). Some researchers also collect real red blood cell images from hospitals. Generally, real images are employed to compute the performance of detection/ segmentation/ classification. The main objective of the research is to formulate effective algorithms for the enhancement/ restoration, segmentation, and classification of sickle cell disease which helps the physician in disease diagnosis as well as in treatment planning.

C. Performance measures

In this section, we concentrate on different performance measures, which are employed for quantitative performance analysis of sickle cell segmentation/ classification. The statistical measures depend on True Positive (TP), False Positive (FP), True Negative (TN) and False Negative (FN). TP illustrates the number of accurately detected unhealthy RBCs (sickle cells). TN characterizes the number of properly detected healthy RBCs. FP is the number of healthy RBCs wrongly detected as unhealthy RBCs (sickle cells) whereas FN represents the number of unhealthy RBCs (sickle cells) incorrectly identified as healthy RBCs. The performance measures are represented as follows.

1) Sensitivity: Sensitivity [128] is represented as a ratio of perfectly classified unhealthy cells (TP) among all unhealthy cells (TP+FN). It is also known as recall, true positive rate (TPR) or the probability of detection. It is mathematically represented as:

$$Sensitivity = \frac{TP}{TP + FN} \tag{7}$$

A method has a relatively high sensitivity means it can classify unhealthy cells better than other methods.

2) Specificity: Specificity is characterized as a ratio of accurately classified healthy cells (TN) among all healthy cells (TN+FP). It is also known as the true negative rate. It is represented as:

$$Specificity = \frac{TN}{TN + FP} \tag{8}$$

A method has relatively high specificity means it can classify healthy cells better than others. Hence, we prefer the method, which has maximum sensitivity and specificity.

3) Accuracy: Accuracy is characterized as a ratio of perfectly classified cells to a total number of cells classified. It is a measure of overall system performance. It is defined as:

$$Accuracy = \frac{TP + TN}{TP + TN + FP + FN} \tag{9}$$

4) Precision: Precision is a ratio of accurately classified unhealthy cells (TP) to all detected unhealthy cells (TP+FP). It is also known as positive predictive value (PPV). It is represented as:

$$\Pr ecision = \frac{TP}{TP + FP} \tag{10}$$

5) F1 Score: F1 Score is the harmonic mean of sensitivity and precision. It is mathematically represented as:

$$F1 \quad Score \quad = \frac{2 \times (Sensitivity \times \Pr ecision)}{(Sensitivity + \Pr ecision)} \tag{11}$$

6) J Score: J Score is also known as Youdens J statistic. It is represented as:

$$J \quad Score \quad = Sensitivity + Specificity - 1 \tag{12}$$

7) False Positive Rate (FPR): FPR indicates the probability of false alarm. It can be evaluated as:

$$FPR = 1 - specificity \tag{13}$$

8) AUC: AUC represents area under the curve: receiver operating characteristic (ROC). ROC is a curve between TPR and FPR at different thresholds. It represents a binary classifiers proper detection capability. AUC ranges between 0 and 1. AUC of an ideal classifier is 1.

VII. Technical Discussion

Accurate detection and classification of sickle cell disease is a tough job in automatic medical diagnosis. In this study, we analyse various techniques for enhancement/ restoration, segmentation, and classification, which is used for the detection of sickle cell disease. Table 1 highlights the strength, weakness, and performance of various methods used by different researchers to diagnose sickle cell disease. The performance analysis of all these methods is a challenging job since different researchers use different datasets, imaging modalities, various segmentations, and validation criteria.

This section highlights the quantitative performance comparison of some of these methods, which is used for the detection of sickle cell disease. It could provide a brief idea about various techniques, which can also be applied for several other applications. From the above analysis, we realize that threshold based segmentation is employed as a preprocessing step before actual segmentation since it is faster and computationally efficient as well. It is very difficult to achieve proper segmentation in the detection of sickle cell disease using a thresholding technique alone since it is independent of the spatial information of images. As thresholding technique only depends on the intensity of pixels, so, it is very sensitive to intensity heterogeneities and noise. Most of the researchers use the watershed algorithm for the segmentation of overlap cells. However, circular Hough transform (CHT) and active contour, particularly the level set method performs better as compared to watershed algorithm. Since CHT emphasizes on circular edge pattern, it is more suitable in the separation of overlapping cells [52, 128, 130, 134]. Region-based techniques, particularly level set method, contour-based method are widely used in the segmentation of blood cells.

We can efficiently segment overlap cells using a level set method with high accuracy, as it is robust to topological variation of the contour. Clustering based techniques like k-means clustering and FCM are most extensively adopted techniques in the segmentation of blood cells from the background.

This article has been accepted for publication in a future issue of this journal, but has not been fully edited. Content may change prior to final publication. Citation information: DOI 10.1109/RBME.2019.2917780, IEEE Reviews in Biomedical Engineering

TABLE I
STRENGTH, WEAKNESS AND PERFORMANCE OF VARIOUS METHODS USED BY DIFFERENT RESEARCHERS FOR THE DIAGNOSIS OF SICKLE CELL DISEASE

Author, Year	Term	Analysis
P. Rakshit and K. Bhowmik 2013 [1]	Strengths	It is computationally efficient and its execution time is small since it only uses Wiener filter, Sobel edge-detector and morphological operator (regionprops) to detect sickle cell.
	Weaknesses	This method does not concentrate on the segmentation of overlapping cell. Thus, it may result false detection. It only emphasizes the detection of sickle cell. However, it does not pay attention to classify it.
	Performance	The proposed method efficiently detects cells with an accuracy of 95.8 %.
Gonzalez-Hidalgo et al. 2013 [2]	Strengths	Here Level set method is employed to generate a contour of an image whereas concave point detection technique is enforced to determine the point of interest. The proposed method [2] utilizes circumference adjustment technique for overlapping circular cells whereas it applies ellipse adjustment technique for overlapping elliptical cells.
	Weaknesses	The input images are not pre-processed. Thus, presence of WBCs and platelets may lead to false detection.
	Performance	It accurately detects circular cells in artificial RBC images with 100% efficiency. It achieves 100% efficiency for the detection of circular cell within a cluster containing two or three overlapping circular cells in real images. This method detects circular as well as elongated RBCs in real images with an efficiency of more than 98%.
Kothari et al. 2009 [7]	Strengths	They have employed concave-point detection and ellipse-fitting approach to properly segment overlapping-cells.
	Weaknesses	It is unable to detect large elongated-cells and large overlapping-cells.
	Performance	It can effectively segment small overlapping-cells with high sensitivity.
Fadhel et al. 2017 [52]	Strengths	CHT based segmentation algorithm is more efficient as well as more robust than Watershed segmentation.
	Weaknesses	Presence of WBCs in an image may lead to false diagnosis as it gives no attention on the elimination of WBCs.
	Performance	For the detection of sickle cell, CHT executes faster than Watershed segmentation.
Sharif et. al. 2012 [53]	Strengths	Marker-controlled watershed can segment small overlapping cells. It can solve the over-segmentation problem.
	Weaknesses	This technique is unable to segment the overlapping RBCs accurately. This approach is somehow able to segment touched cells or overlapping of two cells but unable to segment overlapping of more than two cells.
	Performance	This method is suitable to segment touched cells or overlapping of two cells.
S. S. Savkare and S. P. Narote 2015 [54]	Strengths	K-means clustering is employed to segment the blood cells from the background. Overlapping cells are segmented by using watershed segmentation. Over-segmentation problem can be solved using morphological operations.
	Weaknesses	In low contrast image, K-means clustering is unable to segment cells from background. Post-processing is required as the segmentation of overlapping cells though watershed segmentation faces over-segmentation problem.
	Performance	The segmentation approach successfully segment the cells with 95.5 % accuracy.
Sharma et al. 2016 [56]	Strengths	KNN classifier effectively classifies RBCs into sickle cells, ovalocytes, and dacrocytes. Implementation of KNN classifier is relatively simple and it preserves information in the training phase.
	Weaknesses	The proposed method is unable to segment WBCs from RBCs. This may lead to the false diagnosis of the disease. The response time of KNN classifier is large for huge datasets and it may be sensitive to undesired features.
	Performance	This method classifies sickle cells, ovalocytes, and dacrocytes with 80.6% accuracy and 87.2%, sensitivity.
Tomari et al. 2014 [57]	Strengths	The proposed method uses ANN classifier, which efficiently classifies non-overlap RBCs with 83% accuracy. ANN is capable of providing good performance and it restricts data allocation. This makes ANN more attractive.
	Weaknesses	The proposed method is unable to segment as well as classify overlap cells. The computational complexity of ANN is high, and it has a large response time.
	Performance	This method effectively classifies non-overlap RBCs into healthy and unhealthy cells with an overall accuracy of 83%, average recall of 76% and average precision of 82%.
Khalaf et al. 2017 [58]	Strengths	The proposed method can successfully classify the quantity of medicine dosages required for sickle cell patients.
	Weaknesses	It neither emphasizes analysis of blood cell image to detect sickle-cell nor focuses to classify sickle cell disease.
	Performance	Jordan Neural Network Classifier (JNNC) performs better as compared to other classifiers discussed in this paper with maximum 98.3% training accuracy and 97.2% testing accuracy in class 1.
Khalaf et al. 2016 [59]	Strengths	The proposed method can efficiently classify medicine dosages for sickle cell disease. It may help healthcare organizations to recommend the accurate medicine dosages to sickle cell patients.
	Weaknesses	It only concentrates on the classification of medicine dosages. The proposed method does not pay attention to detection/ segmentation/ classification of RBCs for diagnosis of sickle cell disease using image analysis.
	Performance	H2 classifier achieves maximum 99.5% accuracy whereas H1 classifier achieves 98.8% accuracy.
Xu et al. 2017 [60]	Strengths	Proposed CNN makes feature extraction and classification more robust as well as more efficient. Five-fold cross validation makes the classification more accurate and more reliable.
	Weaknesses	The proposed method is unable to segment overlapped RBCs accurately. It only emphasizes the classification of RBCs into five classes: Echinocytes, Discocytes or Oval, Elongated or Sickle, Reticulocytes and Granular. It does not focus on the classification of sickle cell disease based on the severity of the disease.
	Performance	Deep CNN classifier can efficiently classify RBCs in a robust manner with high accuracy.
Song and Wang 2009 [106]	Strengths	It can successfully segment partially-overlapping cells based on shape information.
	Weaknesses	It is unable to handle over-segmentation and under-segmentation problem.
	Performance	87% of the clusters are segmented successfully. specificity.
Maity et al. 2012 [126]	Strengths	An efficient supervised-decision-tree C4.5 is employed to classify RBCs into six sub-classes including sickle-cells.
	Weaknesses	Presence of overlapping-cells may lead to false diagnosis since it does not segment overlapping-cells accurately.
	Performance	The proposed method efficiently classify RBCs into six sub-classes with 98.2% precision and 99.6% specificity.
Gual-Arnau et al. 2015 [127]	Strengths	They have suggested four features: $W(\phi)$, $W_c(\phi)$, $C_b(\phi)$ and $p(\sigma, \phi)$, which have a vital role in the classification. Finally, they have employed KNN to classify healthy-, sickle-, and other unhealthy-cells.
	Weaknesses	It may demonstrate better performance for the images containing only RBCs. However, in the other images like ErythrocytesIDB database images, the presence of WBCs and platelets may lead to false diagnosis.
	Performance	KNN classifier demonstrates superior performance with $C_b(\phi)$ than other features with 96.16 % overall accuracy.
Elsalamony 2016 [128]	Strengths	It highlights the evaluation of the crucial features: effect-factor and solidity, which differ significantly in healthy- and sickle- cells. Finally, neural-network is employed to detect sickle-cell properly.
	Weaknesses	However, CHT is unable to segment overlapping-cells perfectly due to the elongated nature of RBC.
	Performance	It can successfully detect sickle-cell with unity- specificity, accuracy, and sensitivity.
Acharya and kumar 2017 [129]	Strengths	It can successfully identify 11 sub-classes of RBCs including sickle cells.
	Weaknesses	It is unable to split overlapping cells perfectly, which may cause false diagnosis.
	Performance	The proposed-method perfectly detects 11 sub-classes of RBCs with 98% accuracy.

This article has been accepted for publication in a future issue of this journal, but has not been fully edited. Content may change prior to final publication. Citation information: DOI 10.1109/RBME.2019.2917780, IEEE Reviews in Biomedical Engineering

Author, Year	Term	Analysis
Elsalamony 2017 [130]	Strengths	Here, shape-signature based approach is used to identify sickle-cell. Moreover, back-propagation neural-network is applied to classify healthy- and sickle-cells successfully.
	Weaknesses	CHT is unable to segment overlapping-cells precisely due to the elongated-nature of RBCs.
	Performance	It identifies sickle-cell with unity-accuracy, unity-specificity, and unity-sensitivity.
Maity et al. 2017 [131]	Strengths	The proposed method emphasizes the extraction of crucial shape-based features. Moreover, Adaptive-boosting followed by ensemble-learning are employed to classify RBCs into 9 classes including healthy- and sickle-cells.
	Weaknesses	The proposed method is unable to segment overlapping-cells accurately.
	Performance	It yields superior performance with 99.71% specificity and 97.81% accuracy.
Razzak and Naz 2017 [132]	Strengths	They have proposed a fully-conventional-network based contour-aware-segmentation technique to properly segment overlapping-cells. Moreover, CNN-based-ELM classifier is employed to classify RBCs into 6 subclasses.
	Weaknesses	It does not give priority to classify sickle-cell anemia based on severity of the disease.
	Performance	It can efficiently segment cells with 98.12 % accuracy and 98.36 % precision. Moreover, it can successfully classify RBCs into 6 subclasses with 90.10 % accuracy and 83.14 % precision.
Zhang et al. 2018 [133]	Strengths	A novel U-Net is employed to make the segmentation more accurate and more robust.
	Weaknesses	It pays no attention to the elimination of WBCs, which may lead to false diagnosis.
	Performance	It yields excellent performance with 99.6 % accuracy in single-class RBC segmentation.
Albayark et al. 2018 [134]	Strengths	They have applied CHT to separate healthy-cells from sickle-cells.
	Weaknesses	However, they have not emphasized on the segmentation of overlapping-cells which may lead to false detection. The classification performance can further be improved by employing efficient machine-learning techniques.
	Performance	It classifies healthy- and sickle-cells with 92.9 % precision, 91.11 % accuracy, and 79.05 % recall.
Chy and Rahama 2018 [135]	Strengths	An efficient SVM classifier is employed to classify healthy- and sickle-cells successfully.
	Weaknesses	It gives no importance to segment overlapping cells. analysis.
	Performance	It can successfully classify healthy- and sickle-cells with 95 % accuracy and 96.55 % sensitivity.
Chy and Rahama 2019 [136]	Strengths	Extreme learning machine (ELM), SVM, and KNN are employed to classify healthy- and sickle-cells.
	Weaknesses	It does not emphasize the classification of various stages of sickle cell disease (minor, major, and trait).
	Performance	ELM yields superior performance than KNN and SVM with 87.73% accuracy and 95.45% precision.

For efficient segmentation, an image is pre-processed before the segmentation stage, which enhances the performance of it. The recent advancements in machine learning and deep learning make the feature extraction and classification more popular in medical image analysis for disease diagnosis. Machine learning techniques like KNN [56, 103, 109, 115, 127, 136] and ANN [57] are used for efficient classification of RBCs, which has a vital role in the accurate detection of SCD. Nowadays, deep learning methods especially, CNN and RNN are gaining more importance in medical image analysis [132, 133]. These techniques can dramatically enhance the performance of classification in the detection of SCD.

A. Performance Comparison

Each of the three methods ([2], [8] and [106]) is able to detect artificial-circular-object accurately in an image having two-object clusters. These methods demonstrate excellent performance with 100% efficiency. The detection is based on circumference adjustment technique. Table II represents the detection efficiency of various methods (concave point detection followed by circular adjustment) proposed in [2], [8] and [106] while using artificial images having three-object clusters. Some concave points were falsely identified in Song and Wang [106] proposed method as the estimation of concave points rely on the distance to the skeleton. Moreover, these points may produce invalid lines. Those lines can be treated as valid, especially with noisy contours. It detects the objects with an efficiency of 71.30 % as the concave points are improperly identified. The concave point detection technique proposed by Agam et al. [8] gives false positives due to inaccurate circumference adjustments. However, it achieves 89.16% detection efficiency, which is better than the method proposed by Song and Wang [106].

Gonzalez-Hidalgo et al. [2] have proposed a technique that achieves perfect circular adjustment using artificial images with 100% detection efficiency. The accurate circular adjustment can be achieved due to the correct detection of concave points. The k-curvature technique proposed in [8], may lead to improper detection of the point of interest to circular and elongated objects due to inaccurate local maxima. Since the method proposed in [8] emphasise on curvature variation only in one direction, specious local maxima is detected in the k-curvature for which more numbers of concave points have been identified. However, Gonzalez-Hidalgo et al. [2] focus on the estimation of k-curvatures in both horizontal and vertical directions. Then, they multiply the absolute values these curvatures and identify the concave point based on a threshold. The method proposed in [2] can remove fake concave points successfully by rejecting these points whose multiplication results less than the threshold. Hence, it [2] yields superior performance with high detection accuracy.

TABLE II
DETECTION OF THREE OBJECT CLUSTER USING THE CIRCULAR ADJUSTMENT AND CONCAVE POINT DETECTION METHODS PROPOSED IN [2], [8] AND [106]

Name of the method	Total no. of objects	Objects detected	Efficiency (%)
Concave region extraction and erosion limit [106]	6000	4278	71.30
Chromosome contour extraction, concave point detection and hypothesis verification [8]	6000	5350	89.17
Level set method, Concave point detection and circular adjustment [2]	6000	6000	100.00

The performance of the detection of circular and elongated artificial-objects utilising artificial images of two-object clusters and three-object clusters with ellipse adjustment technique proposed by [2] is illustrated in Table III. In a rare occasion, artificial-objects are overlapped ambiguously and hence, it is

This article has been accepted for publication in a future issue of this journal, but has not been fully edited. Content may change prior to final publication. Citation information: DOI 10.1109/RBME.2019.2917780, IEEE Reviews in Biomedical Engineering

TABLE III
THE DETECTION EFFICIENCY OF ELLIPSE ADJUSTMENT TECHNIQUES PROPOSED IN [2] FOR ARTIFICIAL IMAGES

Type of objects	Two-object clusters			Three-object clusters		
	Objects	Detected objects	Efficiency (%)	Objects	Detected objects	Efficiency (%)
Circular	1975	1949	98.68	2991	2908	97.23
Elongated	2025	1942	95.90	3009	2883	95.81
Circular & elongated	4000	3891	97.28	6000	5791	96.52

TABLE IV
CELL DETECTION IN TWO- AND THREE- CIRCULAR RBCS CLUSTER BY APPLYING THE TECHNIQUES IN [106], [7] AND [2]

Proposed method	Two-RBCs cluster			Three-circular- cluster		
	[106]	[7]	[2]	[106]	[7]	[2]
Circular cells	60	60	60	33	33	33
Detected cells	55	60	60	19	30	33
Efficiency (%)	91.67	100.0	100.0	57.58	90.9	100.0

not possible to detect intersection points accurately. Therefore, it is very difficult to detect the artificial-object properly. The detection efficiency of two-object clusters of circular and elongated artificial-objects are 98.68% and 95.90%, respectively. But, the detection efficiency of three-object clusters of circular and elongated artificial-objects are 97.23% and 95.81%, respectively. The proper detection of intersection points may become more challenging while the area of overlapping is large. The three-object cluster has more overlapped area than a two-object cluster. Hence, the detection of intersection points becomes more difficult. So, it achieves better performance for two-object cluster than the three-object cluster [2].

Table IV illustrate the outcomes achieved after using the techniques proposed in [106], [7] and [2] to real images of two- and three- RBC clusters. The method proposed in [106] requires to detect more concave points since the contour has some noise even after filtration. These extra points are harmful as they develop new line divisions and these points become useless for other lines. In noisy contours, invalid lines might be treated as valid. For two-RBC cluster and three-RBC cluster, the technique proposed in [106] achieves 91.67% and 57.58%, respectively. For the method proposed in [7], in spite of ellipse fitting has been used, the technique depends on line segmentation. It gives the better result as compared to method proposed in [106]. For two-RBC cluster, it can accurately detect all the circular cells with 100% efficiency. However, the detection efficiency reduces to 90.90% for three-RBC clusters as this method is also based on line segmentation even if ellipse fitting is used. The algorithm proposed in [2] can accurately detect all the circular RBCs with 100% efficiency for two-RBC cluster and three-RBC cluster as well. Moreover, its performance remains unaffected by the contour noise.

Table V illustrates the outcomes of ellipse adjustment after executing the techniques proposed in [7] and [2] using two-RBC and three-RBC clusters. The technique proposed in [7] can detect healthy RBCs and sickle cells with an efficiency of 83.51% and 71.45%, respectively since it is based on line segmentation and hence it is not suitable for the accurate detection of large elongated cells and overlapping cells as well. The technique proposed in [2] can accurately detect all the sickle cells with 100% efficiency whereas it is able to detect normal cells with an efficiency of 98.97%.

TABLE V
THE DETECTION EFFICIENCY OF ELLIPSE ADJUSTMENT METHODS SUGGESTED IN [7] AND [2]

Proposed method	[7]	[2]
Circular cells	83.51%	98.97%
Elongated cells	71.45%	100.00%

TABLE VI
CONFUSION MATRIX FOR THE DETECTION OF NORMAL AND ELONGATED RBCS USING SYNTHETIC CELL CLUSTERS [2]

	Normal RBCs estimated	Elongated RBCs estimated	Sensitivity	Specificity	Precision
Normal RBCs	612	0	1.00	0.99	0.99
Elongated RBCs	4	359	0.99	1.00	1.00

Table VI illustrates the classification performance of the method proposed by Gonzalez-Hidalgo et al. [2] on a synthetic image. It is focused on the evaluation of the normal and elongated RBCs estimation. In this experiment, the precision of normal RBCs is enhanced to 0.99 since all the normal RBCs are correctly classified whereas only four elongated RBCs are wrongly classified as normal RBCs. The above results indicate that the algorithm proposed in [2] can efficiently detect normal RBCs and sickle cells with high accuracy. It can properly detect the concave points. Moreover, the performance of the method is better than the method proposed in [106] and [7].

Table VII depicts the detection accuracy of the method proposed by Rakshit and Bhowmik [1]. Here, five samples are processed to evaluate the overall accuracy of the system. It can successfully detect sickle cells with an overall accuracy of 95.8%. However, we can achieve more accurate and more reliable results by using a database having a large number of images. From Table VIII we can clearly observe that CHT performs better than the watershed algorithm [52]. The result illustrates that CHT is more robust as well as more efficient as compared to the watershed algorithm due to a proper estimation of healthy cells and sickle cells as well. CHT is

TABLE VII
EVALUATION OF THE SICKLE CELL DETECTION ACCURACY OF THE METHOD PROPOSED BY RAKSHIT AND BHOWMIK [1]

Sample	RBC count	TP	TN	FN	FP	Accuracy	Overall accuracy
1	10	3	7	0	0	1.000	
2	29	9	17	1	2	0.897	
3	17	6	10	0	1	0.941	0.958
4	21	4	16	0	1	0.952	
5	14	4	10	0	0	1.000	

This article has been accepted for publication in a future issue of this journal, but has not been fully edited. Content may change prior to final publication. Citation information: DOI 10.1109/RBME.2019.2917780, IEEE Reviews in Biomedical Engineering

TABLE VIII
RBCs COUNT USING WATERSHED AND CHT [52]

Segmentation method	Total number of count	Healthy RBC	Abnormal RBC	Elapsed time in seconds
Watershed	233	123	110	11.74394
CHT	233	138	95	8.710206

TABLE IX
COMPARISON OF FEATURES OF FOUR CLASSES OF RBCs [56]

Class	Effect factor	Variance of radial signature	Aspect ratio
Normal RBC (A)	0.9089	0.0946	1.0283
Sickle-cell (B)	0.2543	0.9266	6.2704
Elliptocyte (C)	0.8215	0.5109	1.8701
Dacrocyte (D)	0.6993	0.5709	1.7334

also faster than the watershed algorithm since on CHT circular contours are generated based on voting patterns and after that, local maxima are selected. However, watershed algorithm needs to detect the local minima from which water-drop flow to desired minima, which is a time-consuming process.

Sharma et al. [56] apply KNN classifier to effectively classify RBCs into four classes such as class A-sickle cells, class B-dacrocytes, class C-elliptocytes, and class D-normal RBCs. The features of these four classes are illustrated in Table IX. Table X represents the confusion matrix of the KNN classifier. Sickle cells, normal RBCs, elliptocytes and dracocytes are accurately detected as well as efficiently classified using the method proposed in [56] with 80.6% classification accuracy.

Xu et al. [60] employ deep CNN to efficiently classify RBCs into five classes: Echinocytes, Discocytes or Oval, Elongated or Sickle, Reticulocytes and Granular in the coarse labelling test. The fluctuation may arise due to over-fitting or over-training and this problem can be solved by optimizing the batch size and employing the dropout scheme proposed in [107]. In this [60] proposed method convolutional layer (p=0.5) is employed prior to dropout layer. Table XI illustrates the variation on train error, test error, loss and execution time corresponding to the number of iterations based on the Exp-1 dataset of [60]. From Table XI we notice that both the training error and loss can be optimized by increasing the number of iterations [60]. In the training phase, the classifier achieves excellent performance [60]. The predictive performance of deep CNN can be efficiently computed by implementing k-fold cross-validation. Xu et al. [60] employed 5-fold cross-validation for the predictive performance evaluation of classifier. The total RBC set is further divided into five subsets, and each subset contains an approximately same number of RBCs. For each fold, one of the subsets is selected as a validation set, whereas remaining subsets are employed for training purposes. Finally, prediction score is evaluated as the mean of validation score of five folds. It enhances the stability as well as the reliability of the classifier. However, the training samples are repeated in the k-fold cross validation. Therefore there is a possibility of more or less biased output (validation score). On the other hand, recently proposed nested cross validation method [125] could be used to overcome this problem. It is more reliable. It is also useful to avoid over-fitting and under-fitting problems [125].

From table XII we observe that the average training accuracy of the classifier with five-folds is 91.01% [60]. The classifier produces minimum train error in fifth fold whereas it has optimum evaluation error in the third fold [60]. Table XIII represents the confusion matrix of RBC classification, which uses coarse-labelled RBC dataset [60]. From the table we observed that the class containing elongated and sickle cell having 93.6 % accuracy. The overall accuracy of deep CNN among five classes is 89.9%.

Xu et al. [60] apply refined-labelled RBC dataset to evaluate the performance of deep CNN classifier, which classifies RBCs into eight classes: echinocytes, discocytes, oval, elongated, sickle, reticulocytes, stomatocyte and granular. They also emphasize 5-fold cross-validation. The classification outcomes are displayed in Table XIV. From the table, we observe that the average training accuracy and average evaluation accuracy are 89.69% and 87.5%, respectively. Table XV illustrates the confusion matrix of refined-labelling RBC classification [60]. The deep CNN classifies RBCs into eight classes with overall accuracy of 88.6%. The overall accuracy in refined-labelling classification is smaller than coarse-labelling [60].

The main objectives of Table XIII and XV are to demonstrate the classification performance using various types of RBCs and to evaluate the overall performance. Moreover, a comparative performance analysis between the classes can be

TABLE X
CONFUSION MATRIX OF KNN CLASSIFIER [56]

	A	B	C	D	Accuracy
A	3	0	0	0	100%
B	0	13	0	1	92.9%
C	0	1	4	0	80.0%
D	0	0	4	5	55.6%
Accuracy	100%	92.9%	50.0%	83.3%	80.6%

TABLE XI
COMPARISONS OF LOSS, TRAIN ERROR, TEST ERROR AND EXECUTION TIME BASED ON NUMBER OF ITERATION [60]

Iteration	Training error	Loss	Test error	Time (s)
25	0.2094	0.5879	0.3500	2528.4
30	0.1598	0.3867	0.2750	2940.1
40	0.1213	0.3637	0.2469	4011.5
60	0.1026	0.2805	0.2094	5869.6

TABLE XII
FIVE-FOLD CROSS VALIDATION TO CLASSIFY RBCs INTO 5 CLASSES [60]

Fold no.	Training set	Evaluation set	Training error (%)	Evaluation error (%)
Fold 1	5664	1416	9.14	10.54
Fold 2	5664	1416	9.07	11.16
Fold 3	5664	1416	8.52	10.08
Fold 4	5670	1410	9.84	11.27
Fold 5	5658	1422	8.39	10.55
Mean accuracy			91.01%	89.28%

This article has been accepted for publication in a future issue of this journal, but has not been fully edited. Content may change prior to final publication. Citation information: DOI 10.1109/RBME.2019.2917780, IEEE Reviews in Biomedical Engineering

TABLE XIII
CONFUSION MATRIX OF RBC CLASSIFICATION BASED ON EXP II DATASET OF [60] (COARSE LABELLING)

	Discocytes or Oval	Echinocytes	Elongated or Sickle	Granular	Reticulocytes	Accuracy (%)
Discocytes or Oval	462	1	15	14	3	93.3
Echinocytes	0	147	8	5	10	86.5
Elongated or Sickle	18	0	417	10	0	93.6
Granular	16	10	0	120	13	75.5
Reticulocytes	0	10	4	0	150	91.5
Accuracy (%)	93.1	87.5	93.8	80.5	85.2	89.9

TABLE XIV
FIVE-FOLD CROSS VALIDATION TO CLASSIFY RBCS INTO 8 CLASSES [60]

Fold no.	Training set	Evaluation set	Training error (%)	Evaluation error (%)
Fold 1	5772	1452	10.15	12.41
Fold 2	5772	1452	11.02	13.23
Fold 3	5772	1452	10.26	12.99
Fold 4	5790	1434	10.13	12.51
Fold 5	5790	1434	9.98	11.38
Mean accuracy			89.69 %	87.50 %

achieved if each class having the same number of cells. Since the number of various types of RBCs may vary image to image, the number of cells in each class may differ.

C4.5 supervised-decision-tree can effectively classify RBCs into six subclasses: teardrop, microcytic, elliptocyte, macrocyte, healthy, and sickle-cell [126]. It demonstrates excellent performance with 98.1 % sensitivity, 98.2 % accuracy, and 99.6 % specificity as shown in Table XVI.

Gual-Arnau et al. [127] have extracted crucial features: UNL-F, Effect-Factor and Elliptical-Shape-Factor (EF-ESF), $W(\phi)$, $W_c(\phi)$, $C_b(\phi)$, and $p(\sigma, \phi)$ for effective classification of RBCs [127]. KNN classifier is employed on each of the six-features individually and finally, there performance are compared. From Table XVII, XVIII, and XIX we observe that KNN classifier demonstrates superior performance while considering $C_b(\phi)$ feature than other five features [127].

In the feature-extraction stage, Elasalamony et al. [130] have extracted geometrical-shape-signature whereas Elasalamony et al. [128] have extracted solidity and effect factor. In both cases ([128], [130]) back-propagation neural-network is employed to detect sickle-cell efficiently. From Table XX, we observe that both methods ([128], [130]) can detect sickle-cell successfully with 100% accuracy, sensitivity, and specificity each.

Archarya and Kumar [129] have emphasized the extraction of crucial features: diameter, deviation, shape-geometric-feature, area-proportion, and form-factor to effectively classify RBCs into 11 subclasses. From the Table XXI we observe that the features selected in [129] demonstrates superior accuracy than others [129]. Maity et al. [131] have employed single-rule-engine, C4.5 decision-tree, and ensemble-learning to classify RBCs into seven subclasses including sickle-cell. Table XXII depicts ensemble-learning demonstrate superior performance than other two classifiers [131].

Table XXIII illustrates that the fully-conventional-network based contour-aware-segmentation can efficiently segment RBCs with 98.12% accuracy and 99.17% recall [132]. Razzak [132] has suggested a CNN-based-ELM classifier to classify RBCs into six subclasses: Normal, Elliptocytes and Ovalocytes (E & O), Burr, Sickle (Sic), Acanthocytes (Acan), and Helmet (Helm). Table XXIV depicts that the proposed classifier can classify normal and sickle-cell with 93.69%, 89.46% accuracy, respectively [132]. Table XXV depicts that the deformable U-Net demonstrates superior performance than region-growing and U-Net with 99.60% accuracy and 96.14% precision [133].

Albayrak et al. [134] have suggested a CHT based detection technique, which detects healthy- and sickle-cells with 91.11% accuracy and 92.9% precision as shown in Table XXVI.

Chy and Rahaman [135] have employed SVM, which can efficiently classify healthy and sickle-cells with 95 % accuracy and 96.55 % sensitivity as shown in Table XXVII. Chy and Rahaman [136] have employed SVM, KNN, and ELM classifiers to classify healthy and sickle-cell. Moreover, they have compared their performance, which is represented in Table XXVII. From the table, we observe that ELM demonstrates superior performance than KNN and SVM [136].

B. Clinical Uses

In this review, we discuss various state-of-the-art methods, which are implemented for the detection of sickle cell disease (SCD). We observe a continuous improvement in research for enhancement or restoration, segmentation, and classification of RBCs to make the detection of sickle cells more robust as well as more accurate. The rapid growth of image processing techniques, particularly machine learning and deep learning techniques motivate researchers to design a point-of-care device for the detection and classification of SCD for real-time applications. However, there are certain challenges like the presence of noise, inhomogeneous intensity, overlap RBCs and lack of standard databases, which are responsible for the degradation in the performance of these techniques. The research will be carried out to enhance the performance of traditional techniques as well as to develop new, more efficient algorithms for the detection of SCD.

Many of the methods available in the literature emphasize on the detection, segmentation, and classification of RBCs. However, no proposed method focuses on the severity of the SCD. So, there is sufficient scope to carry out research to classify SCD based on the severity of the disease which will deliver more accurate and realistic results. It will also help physicians in proper diagnosis and treatment planning of SCD.

This article has been accepted for publication in a future issue of this journal, but has not been fully edited. Content may change prior to final publication. Citation information: DOI 10.1109/RBME.2019.2917780, IEEE Reviews in Biomedical Engineering

TABLE XV
CONFUSION MATRIX OF RBC CLASSIFICATION BASED ON EXP II DATASET OF [60] (REFINED LABELLING)

	Disccytes	Echinocytes	Elongated	Granular	Oval	Reticulocytes	Sickle	Stomatocyte	Accuracy (%)
Discocytes	381	0	1	7	16	0	0	0	94.0
Echinocytes	0	123	2	2	0	10	0	1	89.1
Elongated	5	0	243	8	14	0	18	0	84.4
Granular	0	4	3	100	2	1	0	0	90.9
Oval	12	0	12	1	106	0	0	0	80.9
Reticulocytes	0	6	0	3	0	116	0	0	92.8
Sickle	0	9	15	0	6	0	180	1	85.3
Stomatocyte	0	0	0	0	0	2	2	26	86.7
Accuracy (%)	95.7	86.6	88.0	82.6	73.6	89.9	90.0	92.8	88.6

TABLE XVI
PERFORMANCE OF C4.5 SUPERVISED-DECISION-TREE [126]

Classifier	Specificity	Sensitivity	Precision
C4.5	99.6 %	98.1 %	98.2 %

TABLE XVII
OVERALL CLASSIFICATION-ACCURACY OF KNN CLASSIFIER [127]

EF-ESF	UNL-F	$W_c(\phi)$	$p(\sigma,\phi)$	$W(\phi)$	C_b
79.08%	92.48%	93.91%	94.23%	95.99%	96.16%

TABLE XVIII
COMPARISION OF PRECISION USING KNN CLASSIFIER [127]

Cell Type	UNL-F (%)	EF-ESF (%)	$W(\phi)$ (%)	$W_c(\phi)$ (%)	$p(\sigma,\phi)$ (%)	C_b (%)
Sickle	91.66	94.9	96.69	95.36	95.32	95.09
Normal	92.97	63.9	97.68	93.86	94.39	98.12
Other RBCs	93.50	95.7	94.24	92.80	93.23	95.86

TABLE XIX
COMPARISION OF SPECIFICITY USING KNN CLASSIFIER [127]

Cell Type	UNL-F (%)	EF-ESF (%)	$W(\phi)$ (%)	$W_c(\phi)$ (%)	$p(\sigma,\phi)$ (%)	C_b (%)
Sickle	90.24	97.35	95.96	92.86	93.10	95.48
Normal	90.59	73.05	95.29	92.71	93.18	95.29
Other RBCs	96.87	99.03	96.88	96.39	96.63	97.83

TABLE XX
SICKLE CELL DETECTION PERFORMANCE OF THE METHOD PROPOSED IN [128] AND [130]

Performance	Elasalamony et al. [128]	Elasalamony et al. [130]
Accuracy	100 %	100 %
Sensitivity	100 %	100 %
Specificity	100 %	100 %

TABLE XXI
COMPARISON OF DETECTION ACCURACY OF RBC SUBCLASSES [129]

Image labeling	Gray threshold	Morphological operations and metric value	Method proposed in [129]
83.00%	94.58 %	95.80%	98.00%

TABLE XXII
COMPARISON OF CLASSIFICATION PERFORMANCE [131]

Method	Specificity	Accuracy	Sensitivity	Precision
Single-rule-engine	97.90%	96.25%	95.80%	96.23%
C4.5 decision-tree	98.90%	97.10%	96.00%	97.89%
Ensemble-learning	99.71%	97.81%	97.33%	98.00%

TABLE XXIII
RBC SEGMENTATION PERFORMANCE [132]

TP	TN	FP	FN	Accuracy	Precision	Recall
4219	724	21	42	98.12%	98.36%	99.17%

TABLE XXIV
RBC CLASSIFICATION PERFORMANCE [132]

Performance	Normal	E & O	Burr	Sic	Acan	Helm
Accuracy (%)	93.69	90.00	87.49	89.46	86.94	89.58
Precision (%)	90.67	77.51	74.00	83.19	75.75	78.7

TABLE XXV
PERFORMANCE OF SINGLE-CELL RBC SEGMENTATION [133]

Method	Precision	Accuracy	F1 Score
Region-growing	72.23%	96.80%	0.7036
U-Net	95.45%	99.42%	0.9566
Deformable U-Net	96.14%	99.60%	0.9604

TABLE XXVI
HEALTHY- AND SICKLE-CELL DETECTION PERFORMANCE [134]

TP	TN	FP	FN	Recall	Precision	Accuracy
185	467	14	49	79.05%	92.90%	91.11%

TABLE XXVII
HEALTHY- AND SICKLE-CELL CLASSIFICATION PERFORMANCE [135]

Classifier	Sensitivity	Accuracy
SVM	96.55%	95.00%

TABLE XXVIII
HEALTHY- AND SICKLE-CELL CLASSIFICATION PERFORMANCE [136]

Method	Sensitivity	Accuracy	Precision	Specificity	F1
KNN	75.00%	73.33%	90.00%	66.67%	0.8181
SVM	83.33%	83.33%	95.45%	83.33%	0.8889
ELM	87.50%	87.73%	95.45%	83.33%	0.9130

This article has been accepted for publication in a future issue of this journal, but has not been fully edited. Content may change prior to final publication. Citation information: DOI 10.1109/RBME.2019.2917780, IEEE Reviews in Biomedical Engineering

C. Hardware Implementation

Proper detection of sickle cell disease has a key role in the accurate diagnosis of disease as well as in treatment planning. The design of a point-of-care device for the detection and classification of sickle cell disease for real-time applications needs special care since the majority of techniques faces high computational complexity. In level set techniques the contour of the RBCs is represented by a 2-D function, which relies on the characteristics of the image containing RBCs. Hence, while level-set techniques are implemented in hardware for real-time application in spatial domain with parallel processing, it needs various interpolation operations in each iteration. The major advantage of the level set method over active contour is: the level set method is able to manage topological variation. Region growing technique may be effectively employed with parallel processing and shared memory for the segmentation of sickle cell, which plays a vital role in disease diagnosis for real-time application. Sharing of the memory makes the segmentation faster as it restricts several times reading of a seed from the global memory. On the other hand, special care should be taken so that at a particular time a specific region should access a neighbouring element. Hardware implementation of classical FCM is not preferred for real-time application since it has high computational complexity as the membership functions are computed based on Euclidean distance and for a big database it needs large time. Hence, for real-time applications, we may implement modified FCM, which optimizes the computational time.

Thresholding based techniques are more suitable for parallel processing since segmentation of pixels only depends on the intensity of the pixel and threshold value; however, independent of other pixels. Moreover, it requires comparatively less memory and no synchronization. At the same time, a hardware implementation of it needs special care as it is very sensitive to noise and intensity inhomogeneity.

Feature extraction and classification techniques are more suitable to design a point-of-care device for the detection and classification of sickle cell disease for real-time applications. At the time of image transformation, we need an interpolation operation for hardware implementation. Hardware support interpolation makes the system more efficient. Hardware implementation of KNN is simple since it depends on linear computation. Thus, it is more suitable for parallel processing. For classification purpose, ANN might be preferred since the feed-forward network is employed for hardware implementation. Recently, deep learning [60, 92-97, 132, 133] becomes a preferred approach for segmentation and classification of medical images for real-time applications [124, 138].

Gowda and Rasheed [138] have suggested a hybrid CNN-SVM classifier to identify cancer-cell. It is implemented in hardware using Zync-Soc-FPGA. It is a cost-effective real-time-system, which demonstrates superior performance [138]. Knowlton et al. [139] have proposed a novel approach to identify sickle-cell using smart-phone. Pranneerselvam has suggested an efficient ARM 7 micro-controller-based embedded-system for the diagnosis of SCD [140].

VIII. Scopes for Future Work

The quality of an image can be further enhanced using more efficient pre-processing. The segmentation of overlapping cells can be improved by employing distance regularized level set evolution (DRLSE), FCM or other efficient machine learning or image processing techniques. Research can be carried out to make feature extraction and feature selection more accurate and more robust. Gabor filter, LBP, PCA, LDA, etc. can also be employed for effective feature extraction and feature selection. Classification accuracy can be further improved by boosting the performance of ANN, SVM, RNN, CNN, etc. Moreover, these techniques can be modified to boost the performance of a system. The review may motivate researchers to formulate more efficient algorithms for enhancement, restoration, segmentation, and classification. This may be embedded in a suitable hardware to make a point-of-care device, operating in real-time mode, for diagnosis and treatment planning of SCD.

IX. Conclusion

The contributions of this survey article are manifold. The principal objective of the review is to give an overview of the techniques that are available in the literature for the enhancement, segmentation, feature extraction and classification of the image containing RBCs to detect sickle cell disease. The merits and demerits of the recent methodologies are discussed. It has an important role in diagnosis and overall treatment planning of sickle cell disease. It may create a deeper insight into the analysis of state-of-the-art methods. Various performance measures like sensitivity, specificity, accuracy, precision, F1 score, J score, and AUC are used for the quantitative analysis of these techniques. It could be helpful to the researchers in the comparative analysis of various methods. The survey addressed some of the open problems faced by the clinicians. It focusses how to handle inherent problems with the segmentation of overlapping cells, noise removal and IIH correction. The review also highlights hardware implementation, clinical uses and future scopes.This may help researchers and clinicians in deciding a particular methodology, best suited for detection and analysis of SCD.

References

[1] P. Rakshit, and K. Bhowmik, "Detection of Abnormal Finding in Human RBC in Diagnosing Sickle Cell Anaemia Using Image Processing," *ScienceDirect*, vol. 10, pp. 28-36, 2013.

[2] M. Gonzalez-Hidalgo, F. A. Guerrero-Pena, S. Herold-Garca, A. Jaume-i-Capo, and P. D. Marrero-Fernandez, "Red Blood Cell Cluster Separation from Digital Images for use in Sickle Cell Disease," *IEEE Journal on Biomedical and Health Informatices*, pp. 2168-2194, 2013.

[3] D. Anoragaingrum, "Cell segmentation with median filter and mathematical morphology operation," *Proceeding of the IEEE 10th Int. Conf. Image Analysis and Processing (ICIAP)*, pp. 1043–1046, 1999.

[4] K. Wu, D. Gauthier, and M. D. Leiven, "Live cell image segmentation," *IEEE Trans. on Biomedical Engineering*, vol. 42, pp. 1–12, 1995.

[5] M. B. Jeacocke, and B. C. Lovell, "A Multi-resolution algorithm for Cytological image segmentation," *Proceedings of ANZIIS'94-Australian New Zealnd Intelligent Info. Systems Conf., IEEE*, pp. 322–326, 1994.

[6] H. Choi, and R. G. Baraniuk, Multiscale, "Multiscale Image segmentation using wavelet-domain hidden Markov models," *IEEE Trans. on Image Processing*, vol. 10(9), pp. 1309-1321, Sep., 2001.

[7] S. Kothari, Q. Chaudry, and M. D. Wang, "Automated cell counting and cluster segmentation using concavity detection and ellipse fitting techniques," *IEEE International Symposium on Biomedical Imaging: From Nano to Macro. IEEE*, 2009, pp. 795-798, 2009.

[8] G. Agam, and I. Dinstein, "Geometric separation of partially overlapping nonrigid objects applied to automatic chromosome classification," *IEEE Trans. on Pattern Analysis and Machine Intelligence*, vol. 19, no. 11, pp. 1212-1222, 1997.

[9] J. Huang, "An improved algorithm of overlapping cell division," *Int. Conf. Intelligent Computing and Integrated Systems. IEEE*, pp. 687-691, 2010.

[10] J. Fan, Y. Zhang, R. Wang, and S. Li, "A separating algorithm for overlapping cell images," *Journal of Software Engineering and Applications*, vol. 6, pp. 179-183, 2013.

[11] L. Dora, S. Agrawal, R. Panda, and A. Abraham, "State of the art methods for brain tissue segmentation: A review," *IEEE Rev. in Biomed. Eng.*, vol. 10, pp. 235–249, 2017.

[12] C. Chen, W. Xie, J. Franke, P. A. Grutzner, L. P. Nolte, and G. Zheng, "Automatic X-ray landmark detection and shape segmentation via datadriven joint estimation of image displacements," *Med. Image Anal.*, vol. 18, pp. 487-499, 2014.

[13] Y.Artan,A.Oto, and I. S.Yetik, "Cross-device automated prostate cancer localization with multiparametric MRI," *IEEE Trans. Image Process.*, vol. 12, pp. 5385-5394, Dec. 2013.

[14] S. Liao, and D. Shen, "A feature-based learning framework for accurate prostate localization in CT images," *IEEE Trans. Image Process.*, vol. 21, no. 8, pp. 3546-3559, Aug., 2012.

[15] M. M. Fraz, P. Remagnino, A. Hoppe, B. Uyyanonvara, A. R. Rudnicka, C. G. Owen, and S. A. Barman, "An ensemble classification-based approach applied to retinal blood vessel segmentation," *IEEE Trans. Biomed. Eng.*, vol. 9, no. 9, pp. 2538-2548, Sep., 2012.

[16] L. Wen, X. Wang, Z. Wu, M. Zhou, and J. S. Jin, "A novel statistical cerebrovascular segmentation algorithm with particle swarm optimization," *Neurocomputing*, vol. 148, pp. 569-577, 2015.

[17] J. Yao, "Image processing in tumor imaging," *New techniques in oncologic imaging*, pp. 79-102, 2006.

[18] A. Ramkumar, J. Dolz, H. A. Kirisli, S. Adebahr, T. Schimek-Jasch, U. Nestle, L. Massoptier, E. Varga, P. J. Stappers, W. J. Niessen, and Y. Song, "User interaction in semi-automatic segmentation of organs at risk: A case study in radiotherapy," *Journal of digital imaging*, vol. 29, no. 2, pp. 264–277, Apr., 2016.

[19] M. A. Fischler and R. A. Elschlager, "The representation and matching of pictorial structures," *IEEE Trans. on Computers*, vol. 22, no. 1, pp. 67-92, 1973.

[20] B. Widrow, "The rubber-mask technique," *Pattern Recognition*, vol. 5, pp. 175-211, 1973.

[21] M. Kass, A. Witkin, and D. Terzopoulos, "Snakes: Active contour models," *Int. J. Comput. Vis.*, vol. 1, no. 4, pp. 321-331, 1988.

[22] B. Foster, U. Bagci, A.Mansoor, Z. Xu, and D. J. Mollura, "A review on segmentation of positron emission tomography images," *Comput. Biol. Med.*, vol. 50, pp. 76-96, 2014.

[23] T. F. Chan, and L. A. Vese, "Active contours without edges," *IEEE Trans. Image Process.*, vol. 10, no. 2, pp. 266-277, Feb., 2001.

[24] V. Caselles, R. Kimmel, and G. Sapiro, "Geodesic active contours," *Int. J. Comput. Vis.*, vol. 22, no. 1, pp. 61-79, 1997.

[25] M. Jacob, T. Blu, and M. Unser, "Efficient energies and algorithms for parametric snakes," *IEEE Trans. Image Process.*, vol. 13, no. 9, pp. 1231-1244, Sep. 2004.

[26] W. Kim, and J. J. Lee, "Object tracking based on the modular active shape model," *Mechatronics*, vol. 15, no. 3, pp. 371-402, 2005.

[27] L. Jonasson, P. Hagmann, C. Pollo, X. Bresson, C. R. Wilson, R. Meuli, and J. P. Thiran, "A level set method for segmentation of the thalamus and its nuclei in DT-MRI," *Signal Process.*, vol. 87, pp. 309-321, 2007.

[28] R. H. Davies, C. J. Twining, T. F. Cootes, and C. J. Taylor, "Building 3-D statistical shape models by direct optimization," *IEEE Trans. Medical Imag.*, vol. 29, no. 4, pp. 961-981, Apr. 2010.

[29] M. Saadatmand-Tarzjan, "Self-affine snake for medical image segmentation," *Pattern Recognit. Lett.*, vol. 59, pp. 1-10, 2015.

[30] C. Li, X. Wang, S. Eberl, M. Fulham, Y. Yin, and D. D. Feng, "Supervised variational model with statistical inference and its application in medical image segmentation," *IEEE Trans. Biomed. Eng.*, vol. 62, no. 1, pp. 196-207, Jan., 2015.

[31] P. Mesejo, A.Valsecchi, L. Marrakchi-Kacem, S.Cagnoni, and S. Damas, "Biomedical image segmentation using geometric deformable models and metaheuristics," *Comput. Med. Imag. Graph.*, vol. 43, pp. 167-178, 2015.

[32] A. A. Amini, T. E. Weymouth, and R. C. Jain, "Using dynamic programming for solving variational problems in vision, *IEEE Trans. Patt. Anal. Mach. Intell.*, vol. 12(9), pp. 855-867, 1990.

[33] V. Caselles, F. Catte, T. Coll, and F. Dibos, "A geometric model for active contours," *Numerische Mathematik*, vol. 66, pp. 1-31, 1993.

[34] A. Yezzi, S. Kichenassamy, A. Kumar, P. Olver, and A. Tannenbaum., "A geometric snake model for segmentation of medical imagery," *IEEE Trans. Medical Imag.*, vol. 16, pp. 199-209, 1997.

[35] C. Xu, A. Y. Jr., and J. L. Prince, "On the Relationship between Parametric and Geometric Active Contours," *In Proc. of 34th Asilomar Conf. Signals, Systems, and Computers*, pp. 483–489, October 2000.

[36] R. Adams, and L. Bischof, "Seeded region growing," *IEEE Trans. Pattern Anal. Mach. Intell.*, vol. 16, no. 6, pp. 641-647, Jun. 1994.

[37] A. Mehnert, and P. Jackway, "An improved seeded region growing algorithm," *Pattern Recognit. Lett.*, vol. 18, no. 10, pp. 1065-1071, 1997.

[38] X. Lu, J.Wu, X. Ren, B. Zhang, and Y. Li, "The study and application of the improved region growing algorithm for liver segmentation," *OptikInt. J. Light Electron Opt.*, vol. 125, no. 9, pp. 2142-2147, 2014.

[39] A. S. Sajadi, and S. H. Sabzpoushan, "A new seeded region growing technique for retinal blood vessels extraction extraction," *Journal of Medical Signal and Sensor*, vol. 4, no. 3, pp. 223–230, 2014.

[40] C. Li, R. Huang, Z. Ding, J. C. Gatenby, D. N. Metaxas, and J. C. Gore, "A level set method for image segmentation in the presence of intensity in-homogeneities with application to MRI," *IEEE Trans. Image Process.*, vol. 20, no. 7, pp. 2007-2016, 2011.

[41] C. Li, X. Wang, S. Eberl, M. Fulham, and D. D. Feng, "Robust model for segmenting images with/without intensity inhomogeneities," *IEEE Trans. Image Process.*, vol. 22, no. 8, pp. 3296-3309, Aug. 2013.

[42] Y. Boykov, and V. Kolmogorov, "An experimental comparison of min cut/ max-flow algorithms for energyminimization in vision," *IEEE Trans. Pattern Anal. Mach. Intell.*, vol. 26, no. 9, pp. 1124-1137, Sep. 2004.

[43] L. Grady, "Random walks for image segmentation," *IEEE Trans. Pattern Anal. Mach. Intell.*, vol. 28, no. 11, pp. 1768-1783, Nov. 2006.

[44] N. Outs, "A threshold selection method from gray-level histogram," *IEEE Trans. on Systems, Man and Cybernetics*, vol. 9, pp. 62–66, 1979.

[45] B. Venkatalakshmi, and K. Thilagavathi, "Automatic red blood cell counting using Hough transform," *IEEE Conference on Information and Communication Technology*, pp. 267–271, 2013.

[46] K. J. Shanthi, and M..S. Kumar, "Skull stripping and automatic segmentation of brain MRI using seed growth and threshold techniques," *2007 Int. Conf. Intelligent and Advanced Systems*, pp. 25–28, 2007.

[47] M Boegel, P Hoelter, T Redel, A Maier, J Hornegger, and A. Doerfler, "A fully-automatic locally adaptive thresholding algorithm for blood vessel segmentation in 3D digital subtraction angiography," *2015 37th Annual International Conference of the IEEE Engineering in Medicine and Biology Society (EMBC)*, pp. 2006–2009, Aug., 2015.

[48] L. S. Davis, "A survey of edge detection techniques," *Comput Graph Image Process*, vol. 4, no. 3, pp. 248-270, 1975.

[49] J. Canny, "A computational approach to edge detection," *IEEE Trans. Pattern Analysis Machine Intelligence*, vol. 8, no. 6, pp. 679-698, 1986.

[50] G. Ladani, D. A. Randell, S. Fouad, and A. Galiton, "Automatic thresholding from the gradients of region boundaries," *Journal of Microscopy*, vol. 265, pp. 185–195, 2017.

[51] Z. Ma, J. Tavares, R. Jorge, and T. Mascarenhas, "A review of algorithms for medical image segmentation and their applications to the female pelvic cavity," *Computer Methods in Biomechanics and Biomedical Engineering*, vol. 13, no. 2, pp. 235-246, 2010.

[52] M A Fadhel, A J Humaidi, and S R Oleiwi, "Image processing based diagnosis of sickle cell anemia in erythrocytes," *IEEE Annual Conference on New Treand in Information and Communication Technology Applications*, pp. 203–207, 2017.

[53] J. M. Sharif, M. F. Miswan, M. A. Ngadi, Md. S. Salam, and M. M. A. Jamil, "Red blood cell segmentation using masking and watershed algorithm: A preliminary study," *In Biomedical Engineering: ICoBE 2012 International Conference on IEEE*, pp. 258-262, 2012.

[54] S. S. Savkare, and S. P. Narote, "Blood cell segmentation from microscopic blood image," *International Conference on Information Processing. IEEE*, pp. 502-505, 2015.

[55] K. S. Chuang, H. L. Tzeng, S. Chen, J. Wu, and T. J. Chen, "Fuzzy c-means clustering with spatial information for image segmentation," *Comput. Med. Imag. Graph.*, vol. 30, no. 1, pp. 9-15, 2006.

[56] V. Sharma, A. Rathore, and G. Vyas, "Detection of sickle cell anemia and thalassaemia causing abnormalities in thin smear of human blood sample using image processing," *Proceedings of International Conference on Inventive Computation Technologies (ICICT)*, vol. 3, pp. 1-5, 2016.

[57] R. Tomari, W. N. W. Zakaria, M. M. A. Jamil, F. M. Nor, and N. F. N. Fuad, "Computer aided system for red blood cell classification in blood smear image," *Procedia Computer Science*, vol. 42, pp. 206–213, 2014.

[58] M. Khalaf, A. J. Hussain, R. Keight, D. A. Jumeily, R. Keenan, C. Chalmers, P. Fergus, W. Salih, D. H. Abd, and I. O. Idowu, "Recurrent Neural Network Architectures for Analysing Biomedical Data sets," *10th Int. Conf. Developments in eSystems Engineering*, pp. 232–237, 2017.

[59] M. Khalaf, A. J. Hussain, R. Keight, D. A. Jumeily, R. Keenan, P. Fergus, and I. O. Idowu, "The utilisation of composite machine learning models for the classification of medical datasets for sickle cell disease," *Digital Information Processing and Communications (ICDIPC), 2016 Sixth International Conference on IEEE*, pp. 37–41, 2016.

[60] M. Xu, D. P. Papageorgiou, S. Z. Abidi, M. Dao, H. Zhao, and G. E. Karniadakis, "A deep convolutional neural network for classification of red blood cells in sickle cell anemia," *IEEE PLOS computational biology*, pp. 1–15, 2017.

[61] M. K. Hu, "Visual Pattern Recognition by Moment Invariants," *IRE Trans. Info. Theory*, vol. IT-8, pp. 179–187, 1962.

[62] X. Jiang, R. Zhang, and S. Nie, "Image Segmentation Based on Level Set Method," *2012 International conference on Medical Physics and Biomedical Engineering*, Physics Procedia, vol. 33, pp. 840–845, 2012.

[63] M. R. Pinsky, L. Brochard, and J. Mancebo, "Applied Physiology in Intensive Care Medicine," *Springer*, pp. 229–238, 2007.

[64] C. D. Ruberto, A. Dempster, S. Khan, and B. Jarra, "Analysis of infected blood cell images using morphological operators," *Image and Vision Computing*, vol. 20, pp. 133-146, 2002.

[65] M. A. Luengo-Oroz, J. Angulo, G. Flandrin, and J. Klossa, "Mathematical Morphology in Polar-Logarithmic Coordinates. Application to Erythrocytes Shape Analysis," *Springer-Verlag Berlin Heidelberg*, vol. 3523, pp. 199-205, 2005.

[66] J. W. Bacus, "Quantitative red cell morphology," *Monographs in Clinical Cytology*, vol. 9, pp. 1-27, 1984.

[67] K. Horiuchi, J. Ohata, Y. Hirano, and T. Asakura, "Morphologic studies of sickle erythrocytes by image analysis," *The Journal of Laboratory and Clinical Medicine*, vol. 115, no. 5, pp. 613-620, 1990.

[68] L. L. Wheeless, R. D. Robinson, O. P. Lapets, C. Cox, A. Rubio, M. Weintraub, and L. J. Benjamin, "Classification of red blood cells as normal, sickle, or other abnormal, using a single image analysis feature," *Cytometry*, vol. 17, no. 2, pp. 159-166, 1994.

[69] T. Asakura, T. Hirota, A. T. Nelson, M. P. Reilly, and K. Ohene-Frempong, "Percentage of reversibly and irreversibly sickled cells are altered by the method of blood drawing and storage conditions," *Blood Cells, Molecules, and Diseases*, vol. 22, no. 3, pp. 297-306, 1996.

[70] A. N. Schechter, C. T. Noguchi, and G. P. Rodgers, "Sickle Cell Disease. In: Stomatoyanopoulos," *Molecular Basis of Blood Diseases, Philadelphia, W.B. Saunders*, pp. 179–218, 1987.

[71] R. P. Hebbel, "Beyond hemoglobin polymerization: the red blood cell membrane and sickle cell disease pathophysiology," *Blood*, vol. 77, pp. 214–237, 1991.

[72] W. A. Eaton, and J. Hofrichter, "Sickle cell hemoglobin polymerization," *Adv in Protein Chem.*, vol. 40, pp. 63–279, 1990.

[73] M.-T. Le, T. Bretschneider, C. Kuss, and P. Preiser, "A novel semiautomatic image processing approach to determine plasmodium falciparum parasitemia in giemsa-stained thin blood smears," *BMC Cell Biology*, vol. 9, no. 1, pp. 1–15, 2008.

[74] V. V. Makkapati, and R. M. Rao, "Segmentation of malaria parasites in peripheral blood smear images," *IEEE International Conference on Acoustics, Speech and Signal Processing ICASSP 2009. IEEE, 2009*, pp. 1361-1364, 2009.

[75] S. Eom, S. Kim, V. Shin, and B. Ahn, "Leukocyte segmentation in blood smear images using region-based active contours," *In Proceedings of the 8th International Conference on Advanced Concepts For Intelligent Vision Systems, ser. ACIVS06*, pp. 867-876, 2006.

[76] N. Ritter, and J. Cooper, "Segmentation and border identification of cells in images of peripheral blood smear slides," *Proceedings of the Thirtieth Australasian Conf. Computer Science*, vol. 62, pp. 161-169, 2007.

[77] C. Yao, J. Zhang, and H. Zhang, "Blood cell identification and segmentation by means of statistical models," *In Proceedings of the 7th WSEAS International Conference on Signal Processing, Computational Geometry & Artificial Vision*, ser. ISCGAV07, pp. 177-181, 2007.

[78] H. Berge, D. Taylor, S. Krishnan, and T. S. Douglas, "Improved red blood cell counting in thin blood smears," *IEEE International Symposium on Biomedical Imaging: From Nano to Macro.*, 2011, pp. 204-207, 2011.

[79] D. Frejlichowski, "Pre-processing, extraction and recognition of binary erythrocyte shapes for computer-assisted diagnosis based on mgg images," *In Proceedings of the 2010 International Conference on Computer vision and Graphics: Part I, ser. ICCVG10*, pp. 368–375, 2010.

[80] M. Habibzadeh, A. Krzyzak, and T. Fevens, "Application of pattern recognition techniques for the analysis of thin blood smear images," *J. Med. Informat. Technol.*, vol. 18, pp. 29–40, 2011.

[81] X. Qi, F. Xing, D. J. Foran, and L. Yang, "Robust segmentation of overlapping cells in histopathology specimens using parallel seed detection and repulsive level set," *IEEE Trans. on Biomed. Eng.*, vol. 59, no. 3, pp. 754–765, 2012.

[82] N.-T. Nguyen, A.-D. Duong, and H.-Q. Vu, "Cell splitting with high degree of overlapping in peripheral blood smear," *International Journal of Computer Theory and Engineering*, vol. 3, no. 3, pp. 473–478, 2011.

[83] B.Widrow, and M. A.Lehr, "30 years of adaptive neural networks: perceptrons, madaline and Backpropagation," *Proc. IEEE*, vo1.78, pp. 1415–1442, 1990.

[84] J. A. Sethian, "Level set methods and fast marching methods: evolving interfaces in computational geometry, fluid mechanics, computer vision, and materials science," *Cambridge University Press*, vol. 3, 1999.

[85] R. Kimmel, A. Amir, and A. Bruckstein, "Finding shortest paths on surfaces using level set propagation," *IEEE Trans. Pattern Anal. Mach. Intell.*, vol. 17, no. 6, pp. 635–640, Jun., 1995.

[86] C. Li, C. Xu, C. Gui, and M. D. Fox, "Level set evolution without re-initialization: A new variational formulation," *In Proc. IEEE Conf. Comput. Vis. Pattern Recognit.*, vol. 1, pp. 430–436, 2005.

[87] C. Li, C. Xu, K. Konwar, and M. D. Fox, "Fast distance preserving level set evolution for medical image segmentation," *In Proc. 9th Int. Conf. Control Autom. Robot. Vis.*, pp. 1–7, 2006.

[88] J. J. Rodriguez, and L. I. Kuncheva, "Naive bayes ensembles with a random oracle," *In Lect. Notes in Comput. Sci.*, vol. 4472. SpringerVerlag, pp. 450–458, 2007.

[89] R. Battiti, "First- and second order methods for learning: Between steepest descent and Newtons method," *Neural Computation*, vol. 4, no. 2, pp. 141–166, 1992.

[90] K. R. Sing, "A Comparison of gray-level run length matrix and gray level co-occurrence matrix towards cereal grain classification," , International Journal of Computer Engineering & Technology, vol. 7, pp. 9–17, 2016.

[91] J. Ker, L. Wang, J. Rao, and T. Lim, "Deep Learning Applications in Medical Image Analysis," *IEEE Access*, vol. 6, pp. 9375–9389, 2018.

[92] D. Shen, G. Wu, and H.-I. Suk, "Deep learning in medical image analysis," *Annu. Rev. Biomed. Eng.*, vol. 19, pp. 221–48, Mar., 2017.

[93] H. Greenspan, B. V. Ginneken, and R. M. Summers, "Guest editorial deep learning in medical imaging: Overview and future promise of an exciting new technique," *IEEE Trans. Med. Imag.*, vol. 35, no. 5, pp. 1153–1159, May, 2016.

[94] M. R. Osborne, "Fishers method of scoring," *International Statistical Review*, vol. 86, pp. 271-286, 1992.

[95] O. Ronneberger, P. Fischer, and T. Brox, "U-net: Convolutional networks for biomedical image segmentation," *In Proc. Int. Conf. Med. Image Comput. Comput.-Assist. Intervent.*, 2015, pp. 234–241, 2015.

[96] H. C. Shin, H. R. Roth, M. Gao, L. Lu, Z. Xu, I. Noques, J. Yao, D. Mollura, and R. M. Summers, "Deep convolutional neural networks for computer aided detection: CNN architectures, dataset characteristics and transfer learning," *IEEE Trans. Med. Imag.*, vol. 35, pp. 1285–1298, 2016.

[97] N. Tajbakhsh, J. Y. Shin, S. R. Gurudu, R. T. Hurst, C. B. Kendall, M. B. Gotway, and J. Liang, "Convolutional neural networks for medical image analysis: Full training or fine tuning?" *IEEE Trans. Med. Imag.*, vol. 35, no. 5, pp. 1299–1312, May 2016.

[98] N.H. Harun, Nasir, A.S. Abdul, Mashor, M.Y. Mashor, and R. Hassan, "Unsupervised Segmentation Technique for Acute Leukemia Cells Using Clustering Algorithms," *International Journal of Computer, Electrical, Automation, Control and Information Engineering*, vol. 9, no. 1, 2015.

[99] D. Goutam, and S. Sailaja, "Classification of Acute Myelogenous Leukemia in Blood Microscopic Images Using Supervised Classifier," *International Conference on Engineering and Technology*, Maret., 2015.

[100] V. Ivan, K. Ki-Ryong, L. Suk-Hwan, and M. Kwang-Seok, "Acute Lymphoid Leukemia Classification Using Two-Step Neural Network Classifier," *Frontiers of Computer Vision (FCV), IEEE*, pp. 28–30, 2015.

[101] M. M. Amin, S. Kermani, A. Talebi, and M. G. Oghli, "Recognition of Acute Lymphoblastic Leukemia Cells in Microscopic Images Using K-Means Clustering and Support Vector Machine Classifier," *Journal of Medical Signals and Sensors*, vol. 5, pp. 49–58, 2015.

[102] M. Amin, S. Nasser., S. Kermani, and A. Talebi, "Enhanced Recognition of Acute Lymphoblastic Leukemia Cells in Microscopic Images based on Feature Reduction using Principle Component Analysis," *Frontiers in Biomedical Technologies*, vol. 2, issue 3, Nov., 2015.

[103] H. T. Madhloom, S. A. Kareem, and H. Ariffin, "A Robust Feature Extraction and Selection Method for the Recognition of Lymphocyte Versus Acute Lymphoblastic Leukemia," *Int. Conf. Advanced Computer Science Applications and Technologies*, pp. 26–28, 2013.

[104] M. A. Jaffar, A. A. Mirza, and M. Mahmud, "MR imaging enhancement and segmentation of tumor using fuzzy curvelet," *Int. J. Phys. Sci.*, vol. 6, no. 31, pp. 7242–7246, 2011.

[105] R. Cai, Q. Wu, R. Zhang, L. Fan, and C. Ruan, "Red Blood Cell Segmentation Using Active Appearance Model" *ICSP2012 Proceedings, IEEE*, pp. 1641–1644, 2012.

[106] H. Song, and W. Wang, "A new separation algorithm for overlapping blood cells using shape analysis," *International Journal of Pattern Recognition and Artificial Intelligence*, vol. 23, no. 04, pp. 847–864, 2009.

[107] N. Srivastava, G. E. Hinton, A. Krizhevsky, I. Sutskever, and R. Salakhutdinov, "Dropout: a simple way to prevent neural networks from overfitting," *Journal of Machine Learning Research*, vol. 15, pp. 1929–1958, 2014.

[108] R. C. Gonzalez, and R. E. Woods, "Digital Image Processing. Englewood Cliffs," *NJ, USA: Prentice-Hall*, 2008.

[109] H. N. Murthy, and M. Meenakshi, "ANN, SVM and KNN classifiers for prognosis of cardiac ischemiaA comparison," *Bonfring Int. J. Res. Commun. Eng.*, vol. 5, no. 2, pp. 7–11, 2015.

[110] E. S. A. El-Dahshan, H. M. Mohsen, K. Revett, and A. B. M. Salem, "Computer-aided diagnosis of human brain tumor through MRI:Asurvey and a new algorithm," *Expert Syst. Appl.*, vol. 41, pp. 5526–5545, 2014.

[111] T. N. Cruz, T. M. Cruz, and W. P. Santos, "Detection and classification of mammary lesions using artificial neural networks and morphological wavelets," *IEEE Latin America Trans.*, vol. 16, pp. 926–932, May, 2018.

[112] H. Lee and Y. P. Chen, "Cell morphology based classification for red cells in blood smear images," *Patt. Recogn. Lett.*, vol. 49, pp. 155–161, 2014.

[113] D. A. Orrego, M. A. Becerra, and E. Delgado-Trejos, "Dimensionality reduction based on fuzzy rough sets oriented to ischemia detection," *In Proc. 2012 Annu. Int. Conf. IEEE Eng. Med. Biol. Soc.*, pp. 5282–5285, Aug. 2012.

[114] C. I. Christodoulou, and C. S. Pattichis, "Medical diagnostic systems using ensembles of neural SOFM classifiers," *Electronics Circuit and Systems, Proc. of ICECS 99*, 2002.

[115] N. Nabizadeh, and M. Kubat, "Brain tumors detection and segmentation in MR images: Gabor wavelet vs. statistical features," *Comput. Elect. Eng.*, vol. 45, pp. 286–301, 2015.

[116] J. Liu and H. Zhang, "Image segmentation using a local GMM in a variational framework," *J. Math. Imag. Vis.*, vol. 46, pp. 161–176, 2013.

[117] X. Jia, B. Li, and Y. Liu, "Random oracle model," *Journal of Software*, vol. 23, pp. 140–151, Jan. 2012.

[118] D. Marquardt, "An algorithm for least squares estimation of non-linear parameters," *J. Soc. Ind. Appl. Math.*, pp. 43–141, 1963.

[119] D. Lavanya, and K. U. Rani, "Performance evaluation of decision tree classifiers on medical datasets," *International Journal of Computer Applications*, vol. 26, pp. 1–4, 2011.

[120] L. Breiman, "Random forests," *Machine learning*, vol. 45, no. 1, pp. 5–32, 2001.

[121] B. B. Mishra, and S. Dehuri, "Functional link artificial neural network for classification task in data mining," *Journal of Computer Science*, vol. 3, pp. 948–955, 2007.

[122] M. T. Hagan, and M. B. Menhaj, "Training Feedforward Networks with the Marquardt Algorithm," *IEEE Trans. Neural Network*, vol. 5, no.6, pp. 989–993, 1994.

[123] S. Dehuri, R. Roy, S. B. Cho, and A. Ghosh, "An improved swarm optimized functional link artificial neural network (ISO-FLANN) for classification," *Journal of Systems and Software*, vol. 85, pp. 1333–1345, 2012.

[124] G. Litjens, T. Kooi, B. E. Bejnordi, A. A. A. Setio, F. Ciompi, M. Ghafoorian, J. A. W. M. Laak, B. Ginneken, and C. I. Sanchez, "A survey on deep learning in medical image analysis," *Medical Image Analysis*, vol. 42, pp. 60–88, 2017.

[125] L. Dora, S. Agrawal, R. Panda, and A. Abraham, "Nested cross-validation based adaptive sparse representation algorithm and its application to pathological brain classification," *Expert Systems with Applications*, vol. 114, pp. 313–321, Jul. 2018.

[126] M. Maity, P. Sarkar, and C. Chakraborty, "Computer-assisted approach to anemic erythrocyte classification using blood pathological information," *2012 Third Int. Conf. Emerging Applications of Information Technology*, pp. 116–121, 2012.

[127] X. Gual-Arnau, S. Herold-Garca, and A. Sim, "Erythrocyte shape classification using integral-geometry-based methods," *Medical & Biological Engineering & Computing*, vol. 53, pp. 623–633, 2015.

[128] H. A. Elsalamony, "Healthy and unhealthy red blood cell detection in human blood smears using neural networks," *Micron*, vol. 83, pp. 32–41, 2016.

[129] V. Acharya and P. Kumar. "Identification and red blood cell classification using computer aided system to diagnose blood disorders," *2017 Int. Conf. Advances in Computing, Communications and Informatics (ICACCI), IEEE*, pp. 2098–2104, 2017.

[130] H. A. Elsalamony, "Anaemia cells detection based on shape signature using neural networks," *Measurement*, vol. 104, pp. 50-59, 2017.

[131] M. Maity, T. Mungle, D. Dhane, A. K. Maiti, and C. Chakraborty, "An ensemble rule learning approach for automated morphological classification of erythrocytes," *Journal of Medical Systems*, pp. 41–56, 2017.

[132] M. I. Razzak, and S. Naz, "Microscopic blood smear segmentation and classification using deep contour aware CNN and extreme machine learning," *2017 IEEE Conference on Computer Vision and Pattern Recognition Workshops (CVPRW), IEEE*, pp. 801–807, 2017.

[133] M. Zhang, X. Li, M. Xu, and Q. Li, "RBC Semantic Segmentation for Sickle Cell Disease Based on Deformable U-Net," *International Conference on Medical Image Computing and Computer-Assisted Intervention, Springer*, pp. 695–702, 2018.

[134] B. Albayrak, M. B. Darici, F. Kiraci, A. S. renci, A. zmen, and K. Ertez, "Orak Hcreli Anemi Tespiti Sickle Cell Anemia Detection," *Medical Technologies National Congress (TIPTEKNO), IEEE*, pp. 1–4, 2018.

[135] T. S. Chy and M. A. Rahaman, "Automatic Sickle Cell Anemia Detection Using Image Processing Technique," *2018 International Conference on Advancement in Electrical and Electronic Engineering (ICAEEE), IEEE*, pp. 1–4, Nov. 2018.

[136] T. S. Chy and M. A. Rahaman, "A Comparative Analysis by KNN, SVM & ELM Classification to Detect Sickle Cell Anemia," *2019 International Conference on Robotics, Electrical and Signal Processing Techniques (ICREST), IEEE*, pp. 455–459, 2019.

[137] M. Yang, K. Kpalma, and J. Ronsin, "A survey of shape feature extraction techniques," 2008.

[138] M. N. Gowda, and A. I. Rasheed, "Hardware Implementation of Hybrid Classifier to Detect Cancer Cells," *2017 14th IEEE India Council International Conference (INDICON)*, pp. 1–5, 2017.

[139] S. M. Knowlton, I. Sencan, Y. Aytar, J. Khoory, M. M. Heeney, I. C. Ghiran, and S. Tasoglu, "Sickle cell detection using a smartphone," *Scientific reports*, 5, no. 15022, 2015.

[140] P. Panneerselvam, "Application of embedded system for a genetic disease, sickle cell anemia," *2014 International Conference on Advances in Electrical Engineering (ICAEE), IEEE*, PP. 1-4, 2014.